

Synthetic Analogues and Reaction Systems Relevant to the Molybdenum and Tungsten Oxotransferases

John H. Enemark* and J. Jon A. Cooney

Department of Chemistry, University of Arizona, Tucson, Arizona 85721

Jun-Jieh Wang and R. H. Holm*

Department of Chemistry and Chemical Biology, Harvard University, Cambridge, Massachusetts 02138

Received March 17, 2003

Contents

1. Introduction	1175
2. Non-Dithiolene Systems	1178
2.1. Systems Related to the Sulfite Oxidase Family	1178
2.1.1. Structural Analogues	1178
2.1.2. Reactivity Analogues	1178
2.1.3. Hydrotris(pyrazolyl)borate Complexes	1179
2.1.4. Other Ligand Systems	1181
2.2. Systems Related to the Xanthine Oxidase Family	1182
2.2.1. [Mo ^{VI} OS] Complexes	1182
2.2.2. Mo=S Complexes	1183
2.3. Systems Related to the DMSO Reductase Family	1183
2.4. Tungsten Complexes	1184
3. Dithiolene Systems	1184
3.1. Molybdenum	1185
3.1.1. Analogues of the Sulfite Oxidase Family Sites	1185
3.1.2. Analogues of the DMSO Reductase Family Sites	1187
3.2. Tungsten	1189
3.2.1. Tungstoenzymes	1189
3.2.2. Analogue Systems	1190
3.3. Mechanistic Aspects of Oxo Transfer	1193
3.4. Relative Reactivity of Molybdenum and Tungsten	1194
3.5. Relation to Enzymes	1196
3.5.1. Structure	1196
3.5.2. Function	1196
4. Acknowledgments	1198
5. Abbreviations	1198
6. References	1198

1. Introduction

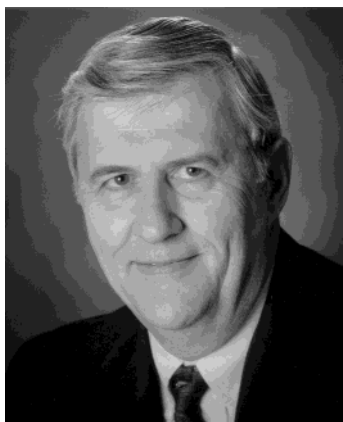
Enzymes containing molybdenum or tungsten at their active sites appear to be present in all forms of life, from ancient archaea to man. These enzymes catalyze a wide range of reactions in carbon, sulfur, and nitrogen metabolism, and at least 50 enzymes are now known.^{1–3} In general, these enzymes utilize

water as the ultimate source or sink of oxygen in the overall catalytic reaction 1, and the reaction coupled



to electron transfer between substrate X/XO, an Fe–S center, heme, or flavin. Representative examples of reactions catalyzed by molybdenum and tungsten enzymes are collected in Table 1. The enzymes are referred to as *oxotransferases* when the substrate is transformed by primary oxygen atom transfer,⁴ and as *hydroxylases* when bound or unbound water or hydroxide is directly involved in the substrate transformation reaction. Among others, the oxidation of sulfite to sulfate and the reduction of Me₂SO to Me₂S can be viewed as oxygen atom (oxo)-transfer reactions. The term “oxotransferase”⁵ is not universally accepted, and the nomenclature of molybdenum and tungsten enzymes and the associated pyranopterindithiolate remains an active area of discussion.⁶

The first crystal structure of a tungsten enzyme appeared in 1995.⁷ Since that time, about 20 X-ray crystal structures of additional molybdenum and tungsten enzymes have been reported.⁸ Further information about the nature of the ligands coordinated to the metal centers has been provided by molybdenum and tungsten XAS investigations. EXAFS analysis generally has afforded more precise metal–ligand bond distances than crystallography. From the combined structural information, Hille^{2,3,9} has classified molybdenum enzymes into three families based upon their protein sequences and the structures of their oxidized active sites. The families are named for their most prominent member. Shown in Figure 1 are schematic representations of active sites in the xanthine oxidase (**2**, **3**), sulfite oxidase (**4**), and DMSO reductase (**5**–**7**) families in the oxidized (Mo^{VI}) and reduced (Mo^{IV}) states. Members of the XnO family are characterized by *one* pyranopterindithiolate entity **1** (also referred to as molybdopterin¹⁰ or pterindithiolene¹¹), which closes a five-membered ene-1,2-dithiolate chelate ring, and a *cis*-Mo^{VI}OS group. The family is represented by aldehyde oxidoreductase^{12–14} and xanthine oxidase/dehydrog-



John H. Enemark grew up in Tyler, MN. He received a B.A. from St. Olaf College (1962) and a Ph.D. from Harvard University (1966), and was a NSF postdoctoral fellow at Northwestern University. Since 1968, he has been a member of the chemistry faculty of the University of Arizona, where he is currently a Regents Professor. In 1974, he and Professor R. D. Feltham developed the widely adopted $\{MNO\}^n$ formalism for describing metal nitrosyl compounds. His present research interests are in bioinorganic chemistry and spectroscopy, with emphasis on molybdenum enzymes and their synthetic analogues.



J. Jon A. Cooney graduated in 1995 from the Imperial College of Science, Technology and Medicine in London, UK, with a degree in chemistry with a Year in Europe. In 1999, he received a Ph.D. from the University of Manchester, UK. His doctoral work, conducted under Professor C. David Garner, was on the chemistry of amavadin, a bioinorganic extract of *Amanita muscaria*. In 2000, he moved to the University of Arizona, where he has since been working as a postdoctoral researcher with Professor Enemark, modeling the active sites of molybdenum and tungsten enzymes.

enase^{2,15–18} with the sites **2ab**. Also classified in this family are certain carbon monoxide dehydrogenases, including that with site **3**. Here, the sulfido ligand is coordinated by Cu^I in what is thus far a unique structure in biology.¹⁹ Chicken liver SO is characterized by *one* ligand **1**, a *cis*- $Mo^{VI}O_2$ group, and a highly conserved cysteinate ligand.^{20–22} Active sites in the SO family, which also includes assimilatory nitrate reductase,²³ are **4ab**. Members of the DMSOR family bind *two* pyranopterindithiolate ligands and in the oxidized forms have one protein ligand and a terminal oxo (as shown) or hydroxo ligand. Among the best characterized structurally are DMSOR from *Rhodobacter sphaeroides* (**5ab**),^{24,25} dissimilatory nitrate reductase from *D. desulfuricans* (**6ab**),²⁶ and formate dehydrogenases from *Escherichia coli*.^{27,28} Sites **7ab** were crystallographically determined. A modified oxidized site has been detected by Se EXAFS, in which selenocysteinyl and one pyranopterindithio-



Jun-Jieh Wang is a native of Taipei, Taiwan, ROC. He is a graduate of National Chung-Hsing University (B.S.) and National Taiwan University (M.S.), has served in the ROC Air Force, and is currently in the doctoral program in chemistry at Harvard University. His research interests include coordination chemistry (with Han-Mou Gau, NCHU), organometallic chemistry (with Ying-Chih Lin, NTU), and bioinorganic chemistry (with R. H. Holm, Harvard University). In college, he sang as a tenor on stage and was an infielder on the school's baseball team. He now spends his leisure time singing karaoke and playing softball.



Richard H. Holm was born in Boston, MA, spent his younger years on Nantucket Island and Cape Cod, and graduated from the University of Massachusetts (B.S.) and Massachusetts Institute of Technology (Ph.D.) He has served on the faculties of the University of Wisconsin, Massachusetts Institute of Technology, and Stanford University. Since 1980, he has been at Harvard University, where he has been Chair of the Department of Chemistry and, from 1983, Higgins Professor of Chemistry. His research interests are centered in inorganic and bioinorganic chemistry, with particular reference to the synthesis and properties of molecules whose structures and reactions are pertinent to biological processes.

late ligand are connected by an Se–S bond (2.12 and 2.19 Å in two different enzymes).^{29,30} The reduced forms of enzymes in the DMSOR family are characterized by desoxo structures (no $Mo=O$ group), unlike those in the other families.³⁰ Structurally characterized tungsten enzymes contain two pyranopterindithiolate ligands per metal atom.^{31,32}

Prior to the availability of detailed knowledge of active site structures, extensive research was performed on molybdenum-mediated oxo transfer,^{4,33,34} often with the explicit desire that it ultimately be relevant to enzyme action. One highly significant consequence of that research and continuing investigations is that the atom-transfer chemistry of molybdenum is the best defined—synthetically, structurally, and mechanistically—of any element. Nearly all early studies focused on the minimal primary oxo-

Table 1. Representative Examples of the Reactions Catalyzed by Molybdoenzymes

enzyme	reaction catalyzed
carbon monoxide oxidoreductase (dehydrogenase)	$\text{CO} + \text{H}_2\text{O} \rightleftharpoons \text{CO}_2 + 2\text{H}^+ + 2\text{e}^-$
dimethyl sulfoxide reductase	$\text{Me}_2\text{SO} + 2\text{H}^+ + 2\text{e}^- \rightleftharpoons \text{Me}_2\text{S} + \text{H}_2\text{O}$
nitrate reductase	$\text{NO}_3^- + 2\text{H}^+ + 2\text{e}^- \rightleftharpoons \text{NO}_2^- + \text{H}_2\text{O}$
arsenite oxidase	$\text{H}_2\text{AsO}_3^- + \text{H}_2\text{O} \rightleftharpoons \text{HAsO}_4^{2-} + 3\text{H}^+ + 2\text{e}^-$
sulfite oxidase	$\text{SO}_3^{2-} + \text{H}_2\text{O} \rightleftharpoons \text{SO}_4^{2-} + 2\text{H}^+ + 2\text{e}^-$
xanthine oxidase	$\text{xanthine} + \text{H}_2\text{O} \rightleftharpoons \text{uric acid} + 2\text{H}^+ + 2\text{e}^-$
aldehyde oxidoreductase	$\text{RCHO} + \text{H}_2\text{O} \rightleftharpoons \text{RCO}_2\text{H} + 2\text{H}^+ + 2\text{e}^-$

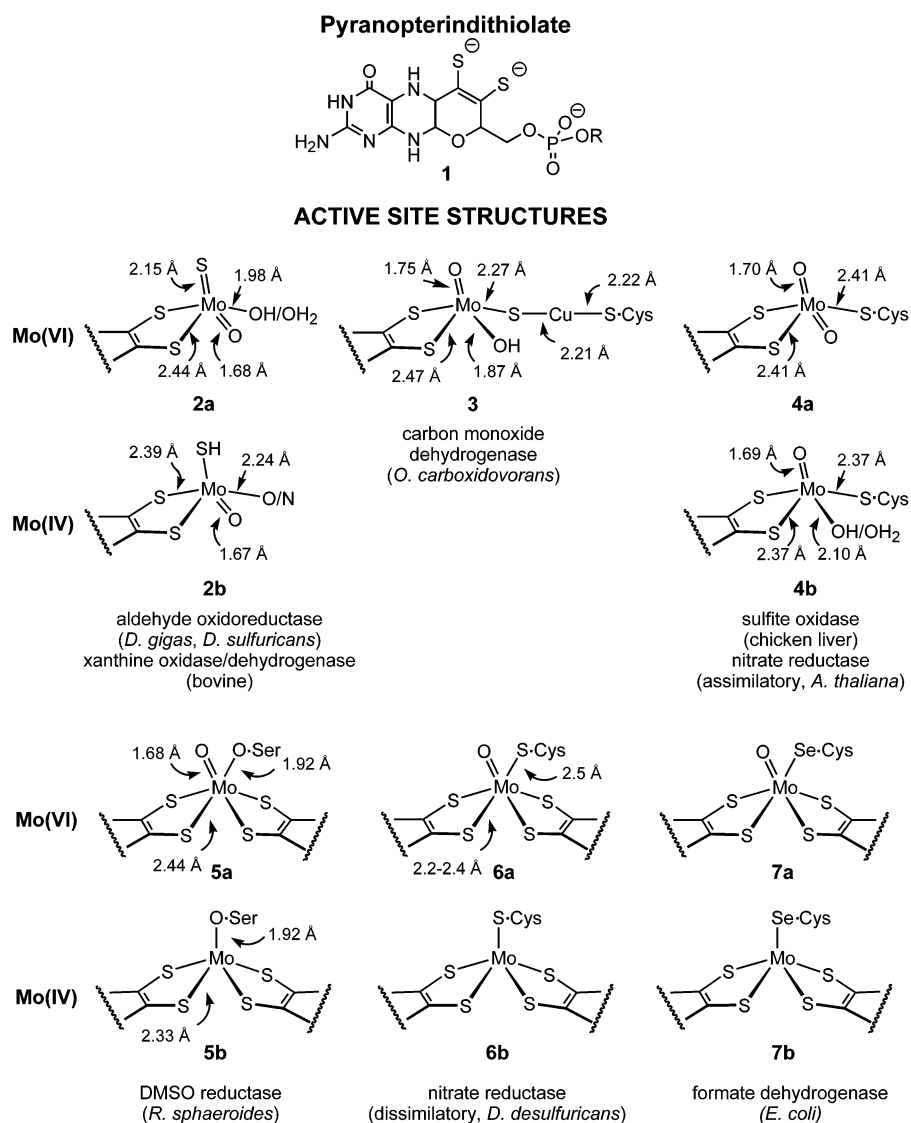
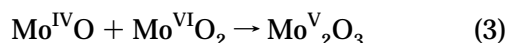


Figure 1. Structure of pyranopterindithiolate (**1**, R absent or a nucleotide) and schematic active site structures of members of the xanthine oxidase (**2**, **3**), sulfite oxidase (**4**), and DMSO reductase (**5**–**7**) enzyme families. Except for **6a**, bond lengths are from EXAFS determinations.

transfer reaction 2, in which atom transfer proceeds by direct interaction of substrate and metal center. Systems that were intended to be biologically realistic were sterically constructed so as to repress or eliminate the usually irreversible μ -oxo “dimerization” reaction 3. At that time, the reaction couple $\text{Mo}^{\text{IV}}\text{O}/$



$\text{Mo}^{\text{VI}}\text{O}_2$ was a natural choice because of the high frequency of occurrence of these groups in conven-

tional molybdenum chemistry. The need to utilize the $\text{Mo}^{\text{IV}}/\text{Mo}^{\text{VI}}\text{O}$ couple became evident only after site structures were known. The structures of Figure 1 pose additional challenges for the synthetic bioinorganic chemist in that several of the features of these centers were not known for complexes of molybdenum prior to the determination of the enzyme crystal structures. Specific synthetic problems are (i) formation of the uncommon $\text{Mo}^{\text{VI}}\text{OS}$ group in the ligand environment of site **2a**; (ii) stabilization of the five-coordinate $\text{Mo}^{\text{VI}}\text{O}_2$ center **4a** of sulfite oxidase in the presence of a strongly reducing ligand environment of three thiolates; and (iii) synthesis of monooxo and

desoxo sites with appropriately simulated protein ligands, there being little or no precedent for these structures. These challenges also apply to the synthesis of analogues of tungstoenzyme sites. The pyranopterindithiolate ligand **1** itself provides an additional synthetic challenge beyond the immediate coordination sphere, although recently the ligand has been synthesized in protected form.³⁵ Synthetic analogues of the pyranopterin have been previously reviewed^{36,37} and are not considered here.

This review will focus primarily on research that has appeared since the structures of the active sites of representative enzymes have become known, i.e., research since about 1995. Existing sources^{4,33,34,37–44} provide background to earlier work in this area. The enzymology and other aspects of molybdenum and tungsten enzymes have been extensively considered elsewhere^{1–3} and are beyond the purview of this review. Chemical approaches to molybdenum and tungsten enzyme sites have been directed toward mimicking a portion of the structural center in order to ascertain the role of that particular feature of the center on the chemical reactivity and the spectroscopic properties of the center. Here we attempt to dissect the contributions of the various features of each site as well as analyze the overall progress on synthetic analogues of these enzyme centers. The discussion is divided into two main parts. The first part deals with systems in which coordination spheres contain nonphysiological ligands and manifest the effects of ene-1,2-dithiolate ligands on the electronic structure of the metal center. The second describes molecules which contain one or two ene-1,2-dithiolate ligands and, where appropriate, simulated protein ligands, and are closer approaches to the sites in Figure 1. For simplicity in nomenclature, we refer to non-dithiolene systems in the first part and dithiolene systems in the second part. *Dithiolene* is a general ligand descriptor widely understood to refer to an ene-1,2-dithiolate or a benzene-1,2-dithiolate dianion in classical complexes, and to a radical monoanion or a dithione in more oxidized molecules. Dithiolenes are notorious noninnocent ligands as in, e.g., the electron-transfer series $[\text{Ni}(\text{S}_2\text{C}_2\text{Me}_2)_2]^{2-,-,0}$ whose two oxidized members have nonclassical electronic structures.⁴⁵ However, in enzymes and their site analogues, all evidence points to a classical description.

Throughout this review we utilize the term “analogue” in describing certain molecules or reaction systems when they resemble or are comparable to enzyme sites and reactions in certain respects. The term is not intended to imply different extents of fidelity to a native property.

2. Non-Dithiolene Systems

2.1. Systems Related to the Sulfite Oxidase Family

Considered here are the structures and properties of various molecules that bear a relationship to the active site of SO, primarily because of the presence

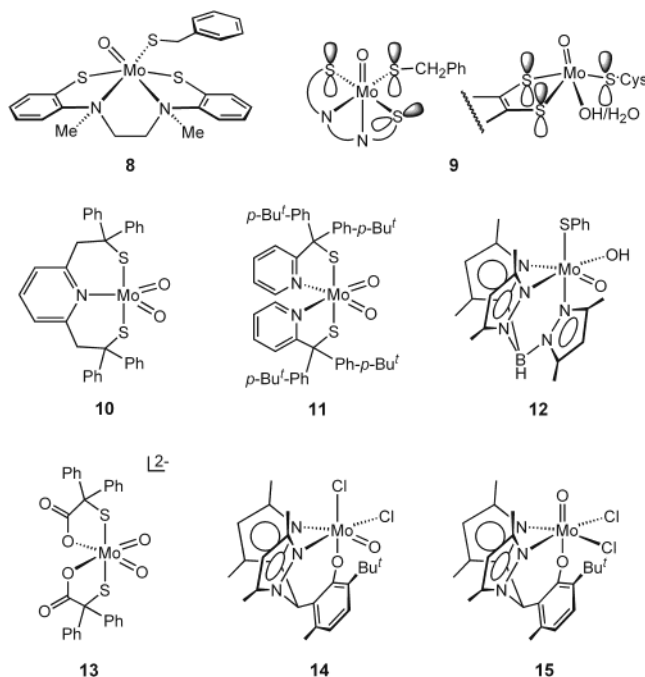


Figure 2. Structures of non-dithiolene oxo-molybdenum complexes.

of the $\text{Mo}^{\text{VI}}\text{O}_2$ group. Structural formulas are set out in Figure 2.

2.1.1. Structural Analogues

The molybdenum center of SO (**4a**, Figure 1) has five-coordinate square pyramidal coordination with three thiolate donors in the equatorial plane, one from a cysteinyl side chain and two from the ene-dithiolate of the pyranopterin moiety.²¹ EXAFS shows that two oxo groups are present in the fully oxidized enzyme.²² This coordination geometry had not been previously seen for a discrete $\text{Mo}^{\text{VI}}\text{O}_2$ molecule. Also having three anionic thiolate donors in the equatorial plane are the *cis,trans*- $[\text{Mo}^{\text{VO}}(\text{L}-\text{N}_2\text{S}_2)(\text{SR})]$ complexes, illustrated with $\text{R} = \text{CH}_2\text{Ph}$ (**8**).⁴⁶ These six-coordinate molecules do not contain an ene-dithiolate ligand in the equatorial plane, but the orientations of the $\text{S}\pi$ orbitals of the monodentate SR ligand and one of the $\text{S}\pi$ orbitals of the $\text{L}-\text{N}_2\text{S}_2$ ligand mimic that of an ene-dithiolate (**9**). The steric constraints of the $\text{L}-\text{N}_2\text{S}_2$ ligand in this isomer^{47–49} orient the third equatorial sulfur atom for participation in strong $d\pi-p\pi$ bonding with the half-filled Mo d_{xy} orbital, and this interaction accounts for the intense absorption of these compounds near 650 nm.^{46,50} The EPR parameters of these complexes more closely approach those of SO than do those of Mo^{VO} compounds with two or four thiolate sulfur atoms in the coordination sphere.⁵¹

2.1.2. Reactivity Analogues

In some respects the chemistry of the SO family should be relatively simple to mimic. The oxidation state changes proposed for the enzymic catalytic cycle are shown in Figure 3. Complexes with the $\text{Mo}^{\text{VI}}\text{O}_2$, Mo^{VO} , and $\text{Mo}^{\text{IV}}\text{O}$ groups are well known.^{52–55} However, oxo-transfer chemistry between substrate and $\text{Mo}^{\text{VI}}\text{O}_2$ or $\text{Mo}^{\text{IV}}\text{O}$ centers in the form of reaction 2 is

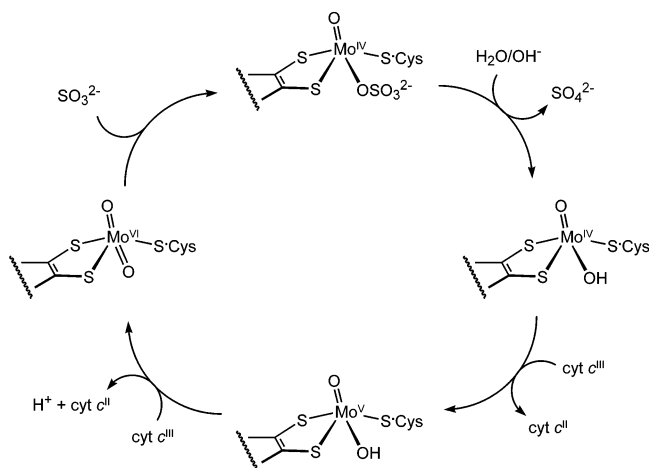
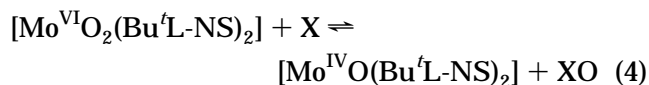


Figure 3. Proposed reaction cycle for sulfite oxidase.

complicated by competing comproportionation reaction 3 to form binuclear $\text{Mo}^{\text{V}}\text{O}$ species containing the $[\text{Mo}_2\text{O}_3]^{4+}$ core.^{4,33,34,56} Similar dimerization reactions can occur for $\text{Mo}^{\text{V}}\text{O}$ centers in the presence of trace amounts of water.³⁴ Thus, an essential requirement for reactivity analogues of sulfite oxidase (and other molybdenum enzymes) is inhibition of the formation of dinuclear Mo^{V} centers. The general approach has been to incorporate steric constraints into the ligands to restrict the approach of the metal centers so that the equilibrium of reaction 3 will lie far to the left. One of the first sulfur-containing ligands to be specifically designed to favor oxygen-atom-transfer chemistry while inhibiting dimer formation was described by Berg and Holm.^{5,57} The X-ray structure of $[\text{Mo}^{\text{VI}}\text{O}_2(\text{L-NS})_2]$ (**10**) suggested that dimerization of the molybdenum center would be unlikely. Complex **10** cleanly oxidizes tertiary phosphines and catalyzes the oxidation of Ph_3P to Ph_3PO by Me_2SO . However, subsequent reinvestigation of this system has shown that reorientation of the ligands after oxygen atom transfer does enable a dinuclear Mo_2O_3 center to form, and that the overall stoichiometry of the oxidation of phosphines involves 2 equiv of **10** per equivalent of phosphine.⁵⁸

A second-generation analogue system incorporated sterically encumbered chelating ligands with N/S coordination.^{59,60} The structures of six-coordinate $[\text{Mo}^{\text{VI}}\text{O}_2(\text{Bu}^t\text{L-NS})_2]$ (**11**) and five-coordinate $[\text{Mo}^{\text{IV}}\text{O}(\text{Bu}^t\text{L-NS})_2]$ were both established by X-ray crystallography, and their interconversion by oxo-transfer reaction 4 was demonstrated by ^{18}O labeling experiments. In nonpolar solvents, the $\text{Mo}^{\text{VI}}\text{O}_2$ and $\text{Mo}^{\text{IV}}\text{O}$



complexes did comproportionate to form $\text{Mo}^{\text{V}}_2\text{O}_3$ centers according to eq 3. However, in the polar solvents used for atom-transfer experiments there was no evidence for dimer formation.⁶⁰ This functional analogue system enabled oxo-transfer reactions to be investigated for a wide range of substrates X/XO, including Et_3P , *S*-oxides, *N*-oxides, and Ph_2SeO , and contributed to the development of a thermodynamic scale for oxo transfer.⁶¹ Reaction 4 was

shown to be second-order with an associative transition state; a reaction pathway was proposed on the basis of kinetics data.⁶² These complexes were also instrumental in the initial theoretical analysis of oxo transfer of $\text{Mo}^{\text{VI}}\text{O}_2$ centers by Pietsch and Hall,⁶³ which has been extended subsequently.^{64–66} The theoretical calculations support an associative transition state that proceeds through a two-step mechanism.⁶⁶ The initial step in phosphine oxidation is nucleophilic attack of the phosphine on a π^* $\text{Mo}=\text{O}$ orbital. This weakens that $\text{Mo}-\text{O}$ bond while strengthening the remaining $\text{Mo}=\text{O}$ bond through the “spectator oxo” effect.⁶⁷ Rotation of the R_3PO ligand about the $\text{Mo}-\text{O}$ bond and hydrolysis (or solvolysis) of the phosphine oxide completes the reaction to yield the final $\text{Mo}^{\text{IV}}\text{O}$ product.

2.1.3. Hydrotris(pyrazolyl)borate Complexes

Another family of ligands that minimize comproportionation is the 3,5-disubstituted trispyrazolylborates. The most extensively studied compounds contain the readily accessible hydrotris(3,5-dimethylpyrazolyl)borate ligand (Tp^*). Compounds of the type $[(\text{Tp}^*)\text{Mo}^{\text{VI}}\text{O}_2\text{X}]$ exhibit oxo transfer to phosphines for $\text{X} = \text{Cl}, \text{Br}, \text{OPh}$, and several thiolates.^{68,69} For $\text{X} = \text{SPh}$, the resultant $[(\text{Tp}^*)\text{Mo}^{\text{IV}}\text{O}(\text{SPh})(\text{py})]$ complex has been isolated in the presence of pyridine and structurally characterized. The $\text{Mo}^{\text{IV}}\text{O}$ species can be reoxidized upon addition of Me_2SO , and it has been shown that these compounds catalyze the oxidation of tertiary phosphines to phosphine oxides by Me_2SO .⁷⁰ Even more interesting than this reversible two-electron oxygen-atom-transfer chemistry is the cycle of reactions that is observed when phosphines are reacted with $[(\text{Tp}^*)\text{Mo}^{\text{VI}}\text{O}_2(\text{SPh})]$ in the presence of small amounts of water.^{68,69} These conditions result in the formation of $[(\text{Tp}^*)\text{Mo}^{\text{V}}\text{O}(\text{OH})(\text{SPh})]$ (**12**), which can be detected by its EPR spectrum. Oxidation regenerates the starting $\text{Mo}^{\text{VI}}\text{O}_2$ compound, which can then react with additional phosphine. When the reaction is carried out in labeled water, the label is incorporated into the phosphine. This analogue system remains the only one that catalyzes a two-electron oxidation of the substrate by an oxygen-atom-transfer reaction with the subsequent regeneration of the oxidized molybdenum center by incorporation of water and successive one-electron transfers, passing through Mo^{V} . Thus, this minimal system incorporates the key components of the reaction proposed for SO (Figure 3), in that the oxygen atom that is incorporated into substrate ultimately comes from water and reoxidation of the molybdenum center proceeds through two sequential one-electron steps.

The $[(\text{Tp}^*)\text{Mo}^{\text{VI}}\text{O}_2(\text{SAr})]$ compounds undergo reversible electrochemistry in rigorously anhydrous solvents to give $[(\text{Tp}^*)\text{Mo}^{\text{V}}\text{O}_2(\text{SAr})]^-$ complexes with distinctive EPR spectra.⁷¹ Addition of water leads to protonation of one of the oxo groups to form $[(\text{Tp}^*)\text{Mo}^{\text{V}}\text{O}(\text{OH})(\text{SAr})]$ (**12**), whose EPR spectra show a splitting from the exchangeable proton of $\sim 10 \times 10^{-4} \text{ cm}^{-1}$, a value comparable to that observed for the $\text{Mo}-\text{OH}$ proton in the low-pH form of sulfite oxidase.⁷² The monoanions can also be generated by

reaction of the dioxo compound with Cp_2Co .⁷¹ When Tp^* is replaced by the related tripodal ligand hydrotris(3,5-dimethyl-1,2,4-triazolyl-1-yl)borate (L'), the resultant $[\text{Cp}_2\text{Co}][\text{L}'\text{Mo}^{\text{V}}\text{O}_2(\text{SPh})]$ species was isolated and its X-ray structure determined.^{73,74}

More recent studies of the reaction of $[(\text{Tp}^*)\text{MoO}_2\text{X}]$ ($\text{X} = \text{Cl}, \text{Br}, \text{OPh}, \text{SPh}$) with Ph_3P have detected $[(\text{Tp}^*)\text{MoOX}(\text{OPPh}_3)]$ intermediates by FAB mass spectrometry.⁷⁵ The compound $[\text{L}^{\text{Pr}}\text{MoO}(\text{OPh})(\text{OPEt}_3)]$ has been isolated and its crystal structure determined. These data support the theoretical descriptions for oxygen-atom-transfer reactions with phosphines in $\text{Mo}^{\text{VI}}\text{O}_2$ centers that were discussed above.

In addition to the chemistry described above, reactions of phosphines with $[(\text{Tp}^*)\text{MoO}_2\text{X}]$ and related L^{Pr} complexes can generate other compounds, depending on the solvent. The nascent $\text{Mo}^{\text{IV}}\text{O}$ species abstracts halogen from halogenated solvents to generate $[(\text{Tp}^*)\text{Mo}^{\text{V}}\text{OX}(\text{halogen})]$.^{76,77} This reaction is useful for synthesizing Mo^{VO} complexes with two different halide ligands. Comproportionation to give binuclear compounds with Mo_2O_3 cores has been observed in dry toluene.⁷⁶

The complexes $[(\text{Tp}^*)\text{Mo}^{\text{IV}}\text{O}(\text{S}_2\text{PR}_2)]$ ($\text{R} = \text{Me}, \text{Et}, \text{Pr}^i, \text{Ph}$) possess a bidentate S_2PR_2 ligand and abstract an oxygen atom from Me_2SO or pyridine *N*-oxide to form $[(\text{Tp}^*)\text{Mo}^{\text{VI}}\text{O}_2(\eta^1\text{-S}_2\text{PR}_2)]$ in a bimolecular process.⁷⁸ The reverse reaction of $[(\text{Tp}^*)\text{Mo}^{\text{VI}}\text{O}_2(\eta^1\text{-S}_2\text{PR}_2)]$ with Ph_3P in dry toluene produces $[(\text{Tp}^*)\text{Mo}^{\text{IV}}\text{O}(\text{S}_2\text{PR}_2)]$, but side reactions complicate kinetic analysis. Reduction of $[(\text{Tp}^*)\text{Mo}^{\text{VI}}\text{O}_2(\eta^1\text{-S}_2\text{PR}_2)]$ by HS^- leads to $[(\text{Tp}^*)\text{Mo}^{\text{V}}\text{O}_2(\eta^1\text{-S}_2\text{PR}_2)]^-$, which converts to $[(\text{Tp}^*)\text{Mo}^{\text{V}}\text{OS}(\eta^1\text{-S}_2\text{PR}_2)]^-$. Ferricinium oxidation of $[(\text{Tp}^*)\text{Mo}^{\text{IV}}\text{O}(\text{S}_2\text{PR}_2)]$ in moist solvents produces $[(\text{Tp}^*)\text{Mo}^{\text{VO}}(\text{OH})(\text{S}_2\text{PR}_2)]$. The Mo^{VO} compounds were characterized by EPR spectroscopy. For the analogous tris(isopropylpyrazolyl)borate compound, reaction with boron sulfide produces $[\text{L}^{\text{Pr}}\text{Mo}^{\text{IV}}\text{S}(\text{S}_2\text{PR}_2)]$, which undergoes oxo transfer to give $[\text{L}^{\text{Pr}}\text{Mo}^{\text{VI}}\text{OS}(\eta^1\text{-S}_2\text{PR}_2)]$ species.⁷⁹ Compounds with a $\text{Mo}^{\text{V}}\text{OS}$ core are considered below.

The Tp^* ligand also provides a vehicle for preparing a wide range of stable Mo^{VO} complexes. Indeed, the $[(\text{Tp}^*)\text{MoO}(\text{X})_2]$ complexes provided the first extensive library of monomeric Mo^{VO} species that could be structurally characterized and investigated by EPR.⁸⁰ These compounds clearly showed a correlation of g and $A(^{95}\text{Mo})$ parameters with the nature of X and indicated that SO should have at least two sulfur atoms in the inner coordination sphere. These compounds also provided evidence that ligand-based protons could give the large splittings for exchangeable protons that are observed in SO.⁸⁰

In summary, Tp^* and related tripodal ligands enable stable mononuclear $\text{Mo}^{\text{VI/V/IV}}$ complexes to be isolated. These ligands contain no anionic sulfur donors, but their complexes have mimicked the overall reaction cycle of SO that involves incorporation of oxygen from water into the substrate via both two-electron and one-electron steps (Figure 3).^{68,69} These complexes also provide vehicles for investigating individually the effects of mono- and dithiolate

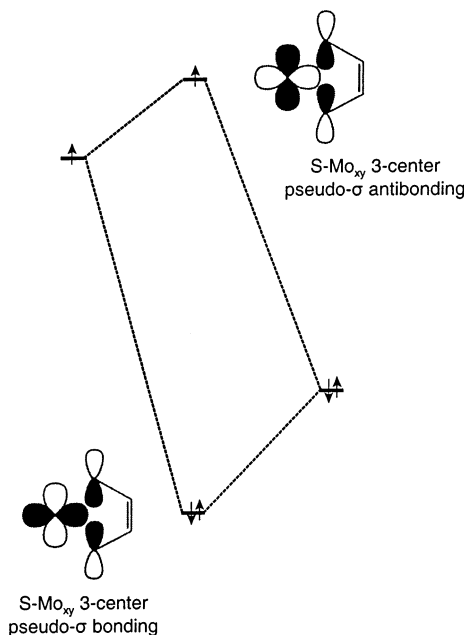


Figure 4. Molecular orbital diagram showing the pseudo- σ -bonding and antibonding interactions of the $\text{Mo } d_{xy}$ and dithiolate ligand orbitals. Adapted with permission from ref 84. Copyright 1999 American Chemical Society.

ligands on the electronic structure of the molybdenum center.

2.1.3.1. Effects of Monothiolate Ligands. The covalency of the $\text{Mo}-\text{SR}$ interaction has been investigated by sulfur K-edge spectroscopy and DFT calculations for $[(\text{Tp}^*)\text{MoO}_2(\text{SR})]$ compounds. It was suggested that the $\text{Mo}-\text{SR}$ torsional angle plays a role in selecting the equatorial oxo group for transfer.⁶⁴ However, Kirk and co-workers⁸¹ have proposed that the primary role of the $\text{Mo}-\text{SR}$ torsional angle is to modulate the potential of the molybdenum site of SO and perhaps provide a superexchange pathway for electron regeneration of the active site. Support for this proposal has been provided by DFT calculations on the SO active-site analogue $[\text{Mo}^{\text{VI}}\text{O}_2\text{-}(\text{S}_2\text{C}_2\text{Me}_2)(\text{SMe})]^-$, which show that at all values of the $\text{O}-\text{Mo}-\text{S}-\text{C}$ dihedral angle, the contribution to the LUMO from the equatorial oxo ligand is 15–20%, substantially greater than that from the axial oxo ligand (<5%).⁸²

2.1.3.2. Effects of Dithiolate Ligands. The contributions of a dithiolate ligand to the electronic structure of an oxo- Mo center have been investigated by MCD, resonance Raman, and electronic absorption spectroscopy of $[(\text{Tp}^*)\text{MoO}(\text{dithiolate})]$ compounds.^{83,84} These studies show that the lowest energy transitions are from out-of-plane filled sulfur $p\pi$ orbitals to the in-plane metal d orbital. The relatively poor overlap makes the bands near $\sim 10\,000\text{ cm}^{-1}$ unusually weak for charge-transfer transitions. The more intense absorption near $\sim 19\,000\text{ cm}^{-1}$ is assigned to a charge-transfer band that involves a pseudo- σ contribution, as shown in Figure 4. This feature mixes in-plane sulfur and molybdenum orbitals and should facilitate electron transfer through the σ -bonding system of the ligand.⁸⁴

The EPR spectra of $[(\text{Tp}^*)\text{Mo}^{\text{VO}}(\text{dithiolate})]$ complexes are essentially identical,^{51,85} as would be

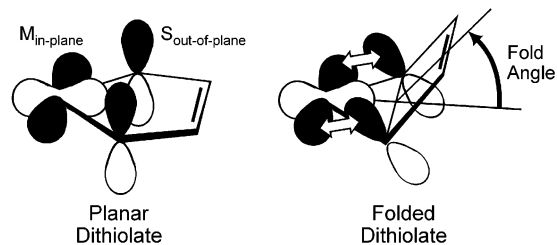


Figure 5. Bonding interaction of the symmetric combination (S_{π^+}) of sulfur out-of-plane orbitals with the metal in-plane d orbitals upon folding of the dithiolate.⁹³

expected, because the EPR parameters are primarily determined by the first coordination sphere of the Mo^{VO} center,⁸⁶ which is the same for these compounds. The electronic effects of dithiolate ligands have also been investigated by gas-phase photoelectron spectroscopy. For $[(\text{Tp}^*)\text{MoE}(\text{tdt})]$ compounds ($E = \text{O}, \text{S}, \text{NO}$), the lowest energy ionization is essentially the same (6.88–6.95 eV), even though the formal d-electron configurations of the metal differ ($4d^1$ for $E = \text{O}, \text{S}$; $4d^4$ for $E = \text{NO}$).⁸⁷ This result contrasts with the PES data for $[(\text{Tp}^*)\text{MoE}(\text{OEt})_2]$ ($E = \text{O}, \text{NO}$), where the NO compound is ~ 0.8 eV more difficult to ionize than the compound with $E = \text{O}$.⁸⁸ These PES results demonstrate the ability of an ene-dithiolate ligand to act as an “electronic buffer” of the charge at the metal center.⁸⁷ For $[(\text{Tp}^*)\text{Mo}^{\text{VO}}(\text{dithiolate})]$ complexes, the lowest energy ionization does show some dependence upon the nature of the arenedithiolate, with compounds possessing electron-withdrawing groups being somewhat more difficult to ionize.^{85,89} In 1,2-dichloroethane solution, cyclic voltammograms of $[(\text{Tp}^*)\text{Mo}^{\text{VO}}(\text{dithiolate})]$ complexes show two reversible waves due to one-electron oxidation and reduction reactions to the corresponding Mo^{VI} and Mo^{IV} species.⁹⁰ The potentials depend on the substituents on the arenedithiolate, and the oxidation potential correlates with the lowest energy gas-phase ionization energy.⁸⁵ The heterogeneous electron-transfer rates are essentially independent of the substituents,⁹⁰ in contrast to the $[(\text{Tp}^*)\text{Mo}^{\text{VO}}(p\text{-OC}_6\text{H}_4\text{X})\text{Cl}]$ and $[(\text{Tp}^*)\text{Mo}^{\text{VO}}(p\text{-OC}_6\text{H}_4\text{X})_2]$ complexes, in which both the potentials and the heterogeneous electron-transfer rates show a dependence on the para substituent of the phenoxy group.⁸⁷ These heterogeneous electron-transfer rate results are consistent with a smaller reorganization energy for electron transfer in $[(\text{Tp}^*)\text{Mo}^{\text{VO}}(\text{dithiolate})]$ compounds compared to $[(\text{Tp}^*)\text{Mo}^{\text{VO}}(p\text{-OC}_6\text{H}_4\text{X})\text{Cl}]$ and $[(\text{Tp}^*)\text{Mo}^{\text{VO}}(p\text{-OC}_6\text{H}_4\text{X})_2]$, which do not have sulfur ligation.

A structural feature of interest for dithiolate complexes is the fold angle of the dithiolate metallacycle along the $\text{S}\cdots\text{S}$ vector. Some years ago it was noted by Lauher and Hoffmann⁹¹ that for $\text{Cp}_2\text{M}(\text{dithiolate})$ compounds, this angle varies with the d-electron configuration of the metal. Compounds with a formal d^0 configuration have large fold angles, whereas those with a d^2 configuration show a fold angle closer to 0° . Large fold angles occur due to the stabilizing interaction of the filled symmetric sulfur $p\pi$ orbital with the empty in-plane metal orbital, as shown schematically in Figure 5. The $[(\text{Tp}^*)\text{Mo}^{\text{VO}}(\text{dithiolate})]$

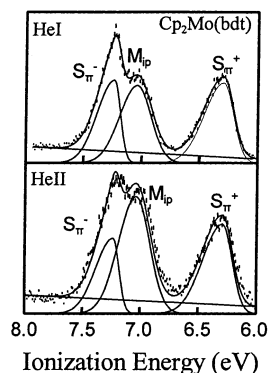


Figure 6. Gas-phase photoelectron spectra of $\text{Cp}_2\text{Mo}(\text{bdt})$ with He^{I} and He^{II} excitation. The substantial relative increase in intensity of the middle peak (M_{π}) upon going from He^{I} to He^{II} excitation indicates that it is primarily metal-based. The lowest energy peak (S_{π^+}) is primarily sulfur, but also has significant metal character.⁹³

complexes have a $4d^1$ electron configuration, and the in-plane metal orbital is singly occupied. Dithiolate fold angles for these compounds range from 6.9 to 29.5° .^{85,92} However, for $(\text{Tp}^*)\text{Mo}(\text{NO})(\text{dithiolate})$ compounds the fold angles are larger (41.4 – 44.4°).⁹³ These large fold angles can be traced back to the electronic structure of the nitrosyl compounds. The presence of the $\{\text{MoNO}\}^4$ group results in the in-plane d_{xy} orbital being empty,⁹⁴ thereby favoring the folding interaction (Figure 5). The availability of planar and folded geometries for dithiolate ligands provides a mechanism for the “electronic buffering” by these ligands,⁸⁷ described above. Figure 6 shows the high-resolution He^{I} and He^{II} gas-phase PES data for $[\text{Cp}_2\text{Mo}(\text{bdt})]$, which has the $4d^2$ electron configuration and nearly planar $\text{Mo}(\text{bdt})$ geometry.⁹⁵ The first (lowest energy) ionization has primarily sulfur character with some additional Mo 4d or C 2p character.⁹³ For $\text{Cp}_2\text{Ti}(\text{bdt})$, which has a “folded” dithiolate geometry and a $3d^0$ electron configuration, the first band shows significantly mixed metal and sulfur character. These gas-phase PES results support substantial covalency for the Mo–S bonds of the dithiolate centers of Figure 1, and it has been suggested that fold angle changes triggered by substrate binding, formation of protein–protein complexes, or protein dynamics may play a role in the catalytic reactions of molybdenum and tungsten enzymes.⁹³

2.1.4. Other Ligand Systems

Cervilla and co-workers⁹⁶ have exploited the sterically hindered 2,2-diphenyl-2-mercaptoacetate ligand to prepare $[\text{Mo}^{\text{VI}}\text{O}_2(\text{O}_2\text{CC}(\text{S})\text{Ph}_2)_2]^{2-}$ (**13**). Reaction of **13** with thiols produces disulfides and 2 equiv of square-pyramidal $[\text{Mo}^{\text{VO}}(\text{O}_2\text{CC}(\text{S})\text{Ph}_2)_2]^-$, which was characterized by X-ray crystallography.⁹⁷ The product Mo^{V} complex is stable in acidic solution, but in neutral solution it slowly converts to the non-oxo $[\text{Mo}^{\text{IV}}(\text{O}_2\text{CC}(\text{S})\text{Ph}_2)_3]^{2-}$, which has trigonal prismatic geometry.⁹⁸ Electrochemical studies in methanol and water show an irreversible proton-assisted reduction to give two Mo^{IV} species, formulated as $[\text{Mo}^{\text{IV}}\text{O}(\text{O}_2\text{CC}(\text{S})\text{Ph}_2)_2]^{2-}$ and $[\text{Mo}^{\text{IV}}\text{O}(\text{O}_2\text{CC}(\text{S})\text{Ph}_2)(\text{solvent})_2]$. Both Mo^{IV} species undergo reversible oxidation to the

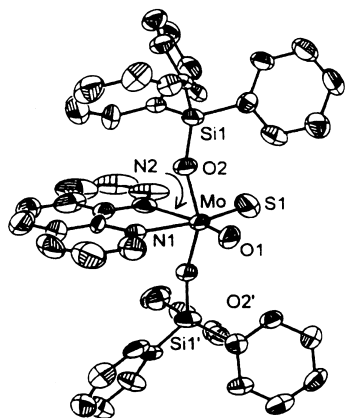


Figure 7. X-ray structure of $[\text{MoOS}(\text{OSiPh}_3)_2(\text{phen})]$ showing 50% probability ellipsoids. Reprinted with permission from ref 104. Copyright 1999 American Chemical Society.

corresponding Mo^{VO} complexes, with no apparent formation of binuclear complexes.⁹⁹ Incorporation of **13** into a layered double-hydroxide host is another strategy for keeping molybdenum reactive centers well separated from one another,¹⁰⁰ and evidence was presented that this system catalyzes the reduction of nitrobenzene to aniline by benzenethiol.¹⁰¹ However, subsequent investigation of this heterogeneous system by XAS suggested that the system contained $\text{Mo}^{\text{VI}}\text{O}_3$ centers.¹⁰²

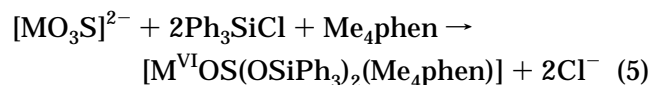
Last, one of the simplest complexes that catalyzes the oxidation of PPh_3 by DMSO is *cis*- $[\text{Mo}^{\text{VI}}\text{O}_2(\text{NCS})_4]^{2-}$, which contains N-bonded thiocyanate ligands.¹⁰³ Stoichiometric oxidation of Ph_3P to Ph_3PO by this anion produces a yellow-red material formulated as $[\text{Mo}^{\text{IV}}\text{O}(\text{NCS})_4]^{2-}$. Comproportionation reaction 3 appears to be inhibited by the anionic nature of both the $\text{Mo}^{\text{VI}}\text{O}_2$ and $\text{Mo}^{\text{IV}}\text{O}$ species.

2.2. Systems Related to the Xanthine Oxidase Family

The oxidized active site of xanthine oxidase/dehydrogenase possesses a terminal oxo group, a terminal sulfido group, one pyranopterindithiolate **1**, and a water or hydroxide ligand (**2a**, Figure 1). The major challenge of incorporating all of these groups on a single molybdenum atom has not yet been met. In this section we address progress on five- and six-coordinate molecules with the *cis*- $[\text{Mo}^{\text{VI}}\text{OS}]^{2+}$ core and those with a single $\text{Mo}=\text{S}$ group.

2.2.1. $[\text{Mo}^{\text{VI}}\text{OS}]$ Complexes

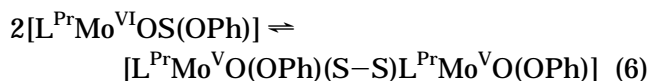
Molecules containing this target group have proved elusive because of the reactivity of the terminal sulfido group. In one approach, using the preformed group in the anions $[\text{MO}_3\text{S}]^{2-}$, the complexes $[\text{M}^{\text{VI}}\text{OS}(\text{OSiPh}_3)_2(\text{Me}_4\text{phen})]$ ($\text{M} = \text{Mo}$,¹⁰⁴ W ¹⁰⁵) are readily prepared by reaction 5; $[\text{Mo}^{\text{VI}}\text{OS}(\text{OSiPh}_3)_2(\text{Me}_2\text{bpy})]$



is available by an analogous method.¹⁰⁴ The crystal structure of $[\text{MoOS}(\text{OSiPh}_3)_2(\text{phen})]$ in Figure 7

exhibits O/S disorder. However, analysis of the EXAFS data at the Mo K-edge clearly showed the presence of both $\text{Mo}=\text{O}$ (1.71 Å) and $\text{Mo}=\text{S}$ (2.19 Å) interactions. Reaction of the $\text{Mo}^{\text{VI}}\text{OS}$ center with Ph_3P resulted in the formation of Ph_3PS and no Ph_3PO , a result that reflects the relative energies of the $\text{Mo}=\text{O}$ and $\text{Mo}=\text{S}$ bonds.¹⁰⁴

The synthesis and properties of $[\text{Mo}^{\text{VI}}\text{OS}]^{2+}$ centers have also been investigated using trispyrazolylborate ligands. Reaction of $[\text{L}^{\text{Pr}}\text{MoO}_2(\text{OPh})]$ with Et_3P , followed by propylene sulfide, generates red-brown $[\text{L}^{\text{Pr}}\text{Mo}^{\text{VI}}\text{OS}(\text{OPh})]$.¹⁰⁶ In the solid state the compound is a dimer which has been shown by X-ray crystallography to contain a disulfido ligand bridging the two molybdenum centers. This species can be viewed as formed by the internal redox⁴² reaction 6. How-



ever, in solution the dimer cleaves, as evidenced by IR bands at 917 and 483 cm^{-1} that are assignable to $\text{Mo}=\text{O}$ and $\text{Mo}=\text{S}$ vibrations, respectively. In addition, the sulfur K-edge XAS spectrum of the solution shows a sharp pre-edge feature characteristic of a transition from the sulfur 1s orbital to the $\text{Mo}=\text{S}\pi^*$ orbital.^{106,107} Electrochemical or chemical reduction of $[\text{L}^{\text{Pr}}\text{Mo}^{\text{VI}}\text{OS}(\text{OPh})]$ affords $[\text{L}^{\text{Pr}}\text{Mo}^{\text{V}}\text{OS}(\text{OPh})]^-$, which is readily protonated to give $[\text{L}^{\text{Pr}}\text{Mo}^{\text{VO}}(\text{SH})(\text{OPh})]$. Solutions of the latter compound exhibit a sharp EPR spectrum with $\langle g \rangle = 1.948$ and $A_{\text{H}} = 11.3 \times 10^{-4} \text{ cm}^{-1}$. Treatment of $[\text{L}^{\text{Pr}}\text{Mo}^{\text{VI}}\text{OS}(\text{OPh})]$ with CN^- in acetonitrile produces $[\text{L}^{\text{Pr}}\text{Mo}^{\text{IV}}\text{O}(\text{MeCN})(\text{OPh})]$ and SCN^- . When the reaction is carried out in moist solvents in the air, the products are $[\text{L}^{\text{Pr}}\text{Mo}^{\text{VI}}\text{O}_2(\text{OPh})]$ and SCN^- .¹⁰⁶ This reaction simulates the deactivation of molybdenum hydroxylases by cyanide.²

Earlier systems with $\text{Mo}^{\text{VI}}\text{OS}$ units include the organometallic compound $[(\text{C}_5\text{Me}_5)\text{MoOS}(\text{CH}_2\text{SiMe}_3)]$,¹⁰⁸ the hydroxylamido complexes $[\text{MoOS}(\text{R}_2\text{NO})_2]$ ($\text{R} = \text{CH}_2\text{Ph}$, Et),^{34,109} bi- and trinuclear oxothiomolybdates(VI),^{110,111} and $[(\text{L}^{\text{Pr}})\text{MoOS}(\eta^1\text{-S}_2\text{-PR}_2)]$.^{79,112} For the latter molecule, the $\text{Mo}=\text{S}$ unit appears to be stabilized by an $\text{S}\cdots\text{S}$ interaction of 2.396(3) Å between the $\text{Mo}=\text{S}$ group and the uncoordinated sulfur of the $\eta^1\text{-S}_2\text{PR}_2$ ligand.

The multiple EPR signals observed for xanthine oxidase in freeze-quench experiments¹¹³ stimulated substantial analogue chemistry, especially by Spence, Wedd, and their co-workers.^{47,114–118} This research has been reviewed previously.³⁴ Reduction of the $\text{Mo}^{\text{VI}}\text{O}_2$ complexes of tetradentate N_2S_2 ligand dianions has produced complexes formulated as containing $[\text{Mo}^{\text{VO}}\text{O}_2]^+$, $[\text{Mo}^{\text{VO}}(\text{OH})]^{2+}$, $[\text{Mo}^{\text{VO}}(\text{OSiMe}_3)]^{2+}$, $[\text{Mo}^{\text{VO}}\text{OS}]^+$, and $[\text{Mo}^{\text{VO}}(\text{SH})]^{2+}$ cores from elegant multifrequency EPR experiments using isotopic labeling with ^{95,97}Mo,⁴⁷ ¹H,⁴⁷ ¹⁷O,¹¹⁵ and ³³S.¹¹⁶ For the complexes of the $[\text{Mo}^{\text{VO}}\text{OS}]^+$ and $[\text{Mo}^{\text{VO}}(\text{SH})]^{2+}$ cores, the Mo K-edge EXAFS and sulfur K-edge XAS data show no evidence for a $\text{Mo}=\text{S}$ bond, but rather are typical of $\text{Mo}-\text{S}$ single bonds to thiolate ligands.⁴⁸ Aqueous micellar solutions of $\text{Mo}^{\text{VI}}\text{O}_2$ complexes of tetradentate N_2S_2 ligands show quasi-reversible electrochemistry with midpoint potentials that decrease linearly

with increasing concentration of DMF and with decreasing pH.¹¹⁹

2.2.2. Mo=S Complexes

An early suggestion that the Mo^V state of XnO possesses a terminal sulfido ligand¹²⁰ stimulated the synthesis of [(Tp*)MoSCl₂] by the reaction of boron sulfide with [(Tp*)MoOCl₂]. Electronic spectra showed that an axial sulfido has a much weaker ligand field than a terminal oxo ligand and that the isotropic *g*-value for the sulfido compound is actually smaller than that for the oxo compound.¹²¹ The sulfur K-edge XAS spectrum of [(Tp*)MoSCl₂] exhibits a sharp pre-edge feature near 2467 eV.⁴⁸ Examples of compounds containing the [Mo=S]³⁺ unit remain relatively rare. Reaction of [(Tp*)MoSCl₂] with anionic monodentate or bidentate ligands produces a variety of [(Tp*)-MoSX₂] complexes, including [(Tp*)MoS(bdt)].¹²¹ All of these compounds exhibit a sharp pre-edge feature in the sulfur K-edge XAS spectrum. The four-coordinate complex [MoS(N[R]Ar)₃] (R = C(CD₃)₂CH₃, Ar = 3,5-C₆H₃Me₂) has been prepared by reacting three-coordinate Mo(N[R]Ar)₃ with S₈.¹²²

From the brief considerations in this section, it is evident that general methods for the formation of Mo^{VI}O_S and Mo^{IV-VI}S groups in desired ligand environments, or the insertion of these groups in such environments, would be a major contribution to synthesis of site analogues of the XnO family.

2.3. Systems Related to the DMSO Reductase Family

A common feature of sites in the DMSOR family is the presence of four thiolate donors from the two pyranopterindithiolate ligands (5–7, Figure 1). Long before the site structure was known, Wedd and co-workers^{123,124} synthesized [Mo^{VO}(SPh)₄]⁻. This intensely blue-colored square pyramidal Mo^V compound stimulated considerable research on [MoO(SAr)₄]⁻ complexes that has been previously summarized.³⁴ These anions and related bidentate dithiolate derivatives¹²⁵ have been important spectroscopic benchmarks for understanding the bonding of Mo^V surrounded by four thiolate sulfur atoms. Electronic absorption, MCD, resonance Raman, and EPR spectra and DFT calculations all support a model in which the unpaired electron is localized in an in-plane orbital that is primarily Mo 4d_{xy} in character and which is well separated from the filled sulfur p orbitals that occur at lower energy.^{81,126} The intense absorption band at ~600 nm results from charge-transfer transitions from the filled sulfur orbitals to this half-filled orbital (SOMO). The structures of these anions have O=Mo–S–C dihedral angles of ~57°.¹²⁴ DFT calculations on [Mo^{VO}(SMe)₄]⁻ show that the total binding energy is minimized at an O=Mo–S–C dihedral angle of 62.8°, similar to the experimental value.¹²⁶ The π-interactions between the filled Sπ orbitals and the in-plane d_{xy} orbital of the metal are very dependent on the dihedral angle.^{81,126} An angle of ~0° maximizes the d_{xy}–Sπ interaction, whereas for a dihedral angle near 90°, as occurs in square pyramidal [Mo^{VO}(dithiolate)₂]⁻ compounds,^{127,128} the energies of the highest occupied

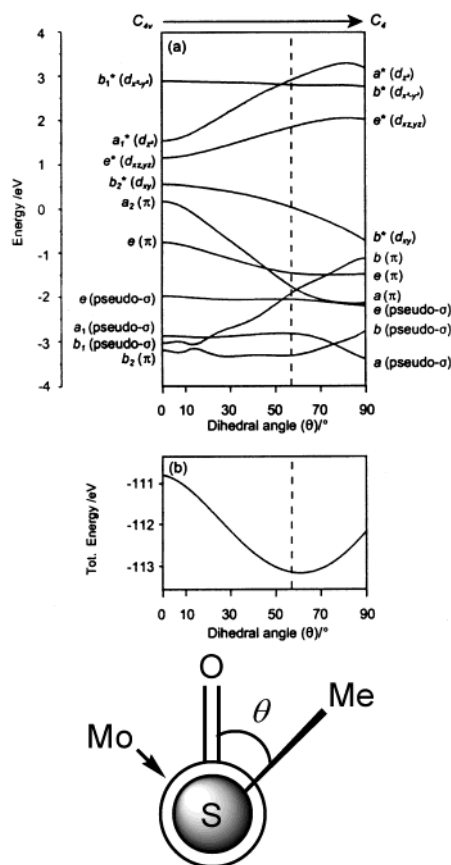


Figure 8. Walsh diagram derived from DFT calculations for [MoO(SMe)₄]⁻, showing (a) the variation in the energy of the frontier orbitals and (b) the variation in total energy as a function of the O–Mo–S–C(R) dihedral angle (θ), which varies between 0° (C_{4v}) and 90° (C_4). The sense of the synchronous rotation of the four MeS ligands used to derive the Walsh diagram is shown by the projection along one of the Mo–S bonds at the bottom of the figure. The $b^*(d_{xy})$ level is the SOMO. The dashed line gives the experimental value of θ for [MoO(SPh)₄]⁻. Adapted with permission from ref 126. Copyright 2001 American Chemical Society.

$S\pi$ orbital and the SOMO become similar. The situation is described by Figure 8. Electronic spectral studies and DFT calculations for [MoO(edt)₂]⁻, which contains bis(dithiolate) coordination, indicate that the SOMO and the filled sulfur π orbitals are much closer together in energy than for [MoO(SPh)₄]⁻ and related complexes of monodentate thiolates.¹²⁶ In fact, unrestricted DFT calculations in rigorous C_{2v} symmetry suggested that the metal-based SOMO was actually slightly lower in energy than the filled $S\pi$ orbitals.¹²⁶

Recent gas-phase anion PES spectroscopy experimentally probed the electronic structures of several compounds with [Mo^{VO}S₄]⁻ coordination.¹²⁹ For [MoO(SPh)₄]⁻ and related complexes of monodentate thiolates, the first ionization can be assigned to a metal-based orbital of Mo^V (4d¹) that is well separated from the filled sulfur p orbitals. However, for [Mo^{VO}(edt)₂]⁻ and other complexes of dithiolate ligands, the first ionization, while still assignable as primarily metal-based, is much closer to the sulfur-based ionizations (Figure 9). The metal nature of the first ionization of [Mo^{VO}(dithiolate)₂]⁻ complexes was experimentally verified by comparison with the analo-

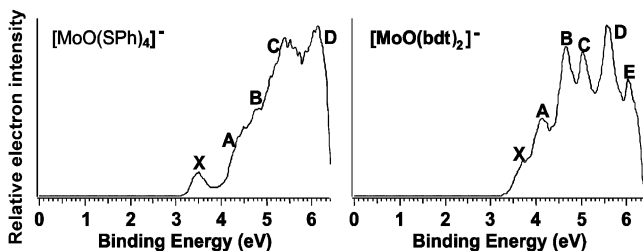


Figure 9. Photoelectron spectra of the $[\text{MoO}(\text{SPh})_4]^-$ and $[\text{MoO}(\text{bdt})_2]^-$ anions at 193 nm (6.424 eV). The peak labeled X is primarily metal based; peaks A–E are primarily sulfur based. Note that the energy separation between X and A is much smaller for the bis(dithiolate) complex. Adapted with permission from ref 129. Copyright 2002 American Chemical Society.

gous $[\text{V}^{\text{VO}}(\text{dithiolate})_2]^-$ complexes. The V^{V} species, which have a $3d^0$ electron configuration, do not show this low-energy feature. DFT calculations reveal that the relative metal and sulfur composition of the highest energy occupied molecular orbital is sensitive to small conformational changes of the dithiolate ligand that substantially improve the overlap of the $\text{S}\pi$ and $\text{Mo } d_{xy}$ orbitals. Thus, the distorted or nonplanar structures observed for $[\text{MoO}(\text{dithiolate})_2]^-$ ^{127,130} may be electronic in origin.¹²⁹ The electronic structure results deduced from the anion PES spectra are complementary to those derived from MCD studies of $[\text{MoO}(\text{bdt})_2]^-$.¹³¹

The electronic and EPR spectra of $[\text{Mo}^{\text{VO}}(\text{SAr})_4]^-$ complexes are relatively insensitive to arene substituents.^{126,132} However, early studies showed a correlation of their $\text{Mo}^{\text{VI/V}}$ and $\text{Mo}^{\text{V/IV}}$ potentials with Hammett parameters of the substituents on the arene thiolate.¹³² Nakamura and co-workers¹³³ showed that the reduced compound $(\text{Et}_4\text{N})_2[\text{Mo}^{\text{VO}}(\text{S}-p\text{-C}_6\text{H}_4\text{Cl})_4]$ exhibits $\text{O}=\text{Mo}-\text{S}-\text{C}$ dihedral angles of $74-91^\circ$, in agreement with extended Hückel molecular orbital calculations. This stereochemistry is topologically similar to that of $[\text{MoO}(\text{dithiolate})_2]^{2-}$ compounds.^{127,128} Incorporation of ortho NH groups into arenethiolate ligands leads to intraligand $\text{N}-\text{H}\cdots\text{S}$ hydrogen bonds and an $\text{O}=\text{Mo}-\text{S}-\text{C}$ dihedral angle of $\sim 0^\circ$, with all of the NH groups pointed toward the terminal oxo group. The $\text{Mo}^{\text{V/IV}}$ reduction potentials of these arenethiolate complexes with ortho amide groups increased by +450 mV relative to that of $[\text{Mo}^{\text{VO}}(\text{SPh})_4]^-$.¹³⁴ More recently, Mondal and Basu¹³⁵ showed that encapsulating a $[\text{Mo}^{\text{VO}}(\text{SAr})_4]^-$ complex into a dendrimer (to mimic the change in dielectric constant and solvent exposure of a protein) increased the $\text{Mo}^{\text{V/IV}}$ potential by ca. 100–300 mV, depending on the solvent. The electronic and EPR spectra were little different from those of the parent $[\text{Mo}^{\text{VO}}(\text{SPh})_4]^-$ anion.^{81,126}

Another structural feature of active sites in the DMSOR family (Figure 1) is the ligand contributed by the protein backbone. For DMSOR itself, this is the oxygen atom of a serinate residue. Other members of the family have sulfur from cysteinate²⁶ or selenium from selenocysteine²⁷ as the additional ligand. Complexes of modified trispyrazolylmethane that contain a phenoxide group on one arm form six-coordinate $[(\text{L}1\text{O})\text{Mo}^{\text{VO}}\text{Cl}_2]$ complexes in which the phenoxide oxygen atom is either cis or trans to the

terminal oxo group (14, 15; Figure 2). The trans isomer is ~ 200 mV easier to reduce. It has been suggested that, in DMSOR, the position of the serinate relative to the oxo group may be important in determining the reduction potential of the site.¹³⁶

Another unusual feature of the DMSOR site is that the oxidized resting state contains the monooxo group $\text{Mo}^{\text{VI}}\text{O}$. The description of the site was initially controversial owing to crystallographic disorder,²⁴ as has been reviewed elsewhere.¹³⁷ The oxygen-atom-transfer chemistry of DMSOR thus involves $\text{Mo}^{\text{VI}}\text{O}$ and desoxo Mo^{IV} centers (vide infra). Six-coordinate complexes containing the monooxo group are rare.¹³⁸ Seven-coordinate species are more common; one instance of oxo-transfer reactivity has been reported.¹³⁹ Recently, Basu and co-workers¹⁴⁰ have shown that oxidation of $[(\text{Tp}^*)\text{Mo}^{\text{VO}}(\text{O}-p\text{-C}_6\text{H}_4\text{OEt})_2]$ by $(\text{NH}_4)_2[\text{Ce}(\text{NO}_3)_6]$ produces a $\text{Mo}^{\text{VI}}\text{O}$ species that undergoes oxo-transfer chemistry with tertiary phosphines. Mass spectral studies showed that, in H_2^{18}O , this system will catalyze the incorporation of ^{18}O into the Ph_3PO product.

2.4. Tungsten Complexes

All known tungstoenzymes have two pyranopterindithiolate ligands.^{8,32} Chemical and EXAFS studies suggest that $\text{W}=\text{O}$, $\text{W}=\text{S}$, and/or $\text{W}-\text{SH}$ groups may also be present.¹⁴¹⁻¹⁴³ Several compounds with these terminal functions have been prepared and investigated. These include the cis,trans forms of $[\text{W}^{\text{VI}}\text{O}_2(\text{L}-\text{N}_2\text{S}_2)]$, $[\text{W}^{\text{VI}}\text{OS}(\text{L}-\text{N}_2\text{S}_2)]$, and $[\text{W}^{\text{VI}}\text{S}_2(\text{L}-\text{N}_2\text{S}_2)]$, *cis,cis*- $[\text{W}^{\text{VI}}\text{OX}(\text{L}-\text{N}_2\text{S}_2)]$, and *cis,trans*- $[\text{W}^{\text{VI}}\text{OX}(\text{L}-\text{N}_2\text{S}_2)]$ ($\text{X} = \text{NCS}^-$, Cl^- , OPh^- , SPh^-) (all from ref 144), $[\text{W}^{\text{VI}}\text{O}_2(\text{O}_2\text{CCSPh}_2)_2]^{2-}$,¹⁴⁵ and $[(\text{Tp}^*)\text{W}^{\text{VI}}\text{OSX}]$ and $[(\text{Tp}^*)\text{W}^{\text{VI}}\text{S}_2\text{X}]$.^{107,146} In general, tungsten complexes are more difficult to reduce than their molybdenum counterparts at parity of ligation.¹⁴⁷ For example, the $\text{W}^{\text{VI/V}}$ and $\text{W}^{\text{V/IV}}$ potentials of $[(\text{Tp}^*)\text{WO}(\text{tdt})]$ are 382 and 272 mV more negative, respectively, than the potentials of the corresponding couples of $[(\text{Tp}^*)\text{MoO}(\text{tdt})]$.⁹⁰ Tungstoenzymes are considered more fully in section 3, together with their bis(dithiolene) site analogues.

3. Dithiolene Systems

The two fundamental types of dithiolene ligands are depicted in their classical, fully reduced forms, ene-1,2-dithiolate (16) and benzene-1,2-dithiolate (17, bdt), in Figure 10. Both ligand types are available with a variety of substituents. While 17 and its derivatives have been isolated in substance as alkali metal salts, only a few isolated compounds of dianion 16 are known. These include ligands with $\text{R} = \text{H}^{148}$ and CN^{149} (mnt) substituents. Those with $\text{R} = \text{alkyl}$, the most physiologically realistic when compared with pyranopterindithiolate 1, are practically unknown in isolated form. One ligand with a bicyclic aliphatic backbone has been prepared as the sodium salt.¹⁵⁰ While not available as reagents, ligands with $\text{R} = \text{alkyl}$ and phenyl substituents are obtainable in protected forms in solution and may be deprotected in the presence of metals to form complexes.¹⁵¹⁻¹⁵⁴ In some cases, the ligand may be transferred from one

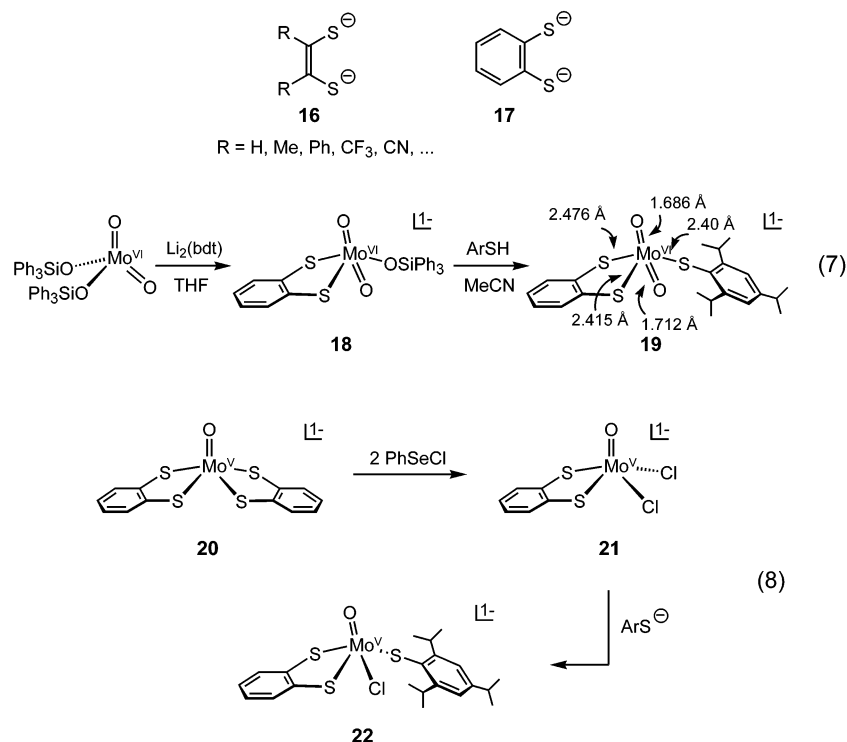


Figure 10. Structures of the two fundamental types of dithiolene ligands in the dithiolate oxidation state (**16**, **17**). The use of the bdt ligand in stabilizing site analogues **19** and **22** in the SO enzyme family is illustrated. Adapted with permission from ref 159. Copyright 2001 American Chemical Society.

metal to another (vide infra). As noted as the outset, the available evidence, particularly structural information, for all analogue complexes in the $M^{\text{IV-VI}}$ oxidation states indicates that ligands function as classical dianions. For example, in $[\text{W}^{\text{VI}}\text{O}(\text{S}_2\text{C}_2\text{Me}_2)_2]^-$, the mean chelate ring C–C (1.329 Å) and C–S (1.790 Å) distances are consistent with standard C=C double bond (1.33 Å) and C–S single bond (1.82 Å) lengths.¹⁵⁵ The principal effect of variant R substituents in **16** is modulation of electron distribution and attendant redox potentials. Given the classical behavior of the ligands, electron-transfer reactions are metal-centered. The effect on potentials can be quite large, as in the couple $[\text{MoO}(\text{S}_2\text{C}_2\text{R}_2)_2]^{-/2-}$, where $\text{R} = \text{Me} (-0.62 \text{ V}) < \text{Ph} (-0.46 \text{ V}) < \text{CF}_3 (0.18 \text{ V}) < \text{CN} (0.48 \text{ V})$ in acetonitrile.^{130,156} (Here and elsewhere, potentials are referenced to the SCE.) Because of the strong inductive effect of the cyano group, the mnt ligand is the least physiological in the set. The ligand with $\text{R} = \text{Me}$ is far more satisfactory in simulating the electron distribution within the chelate rings formed by **1** and, as will be seen, has assumed a prominent role in molybdenum and tungsten analogue chemistry.

Metal dithiolene complexes were first prepared in the early 1960s, and non-innocent ligand behavior in oxidized species was quickly recognized. An account of early developments is available.¹⁵⁷ In the ensuing 20-year period prior to elucidation of the pyranopterin structure by chemical means and the proposed ene-1,2-dithiolate chelation to molybdenum,^{10,158} there was no indication—perhaps not even a hint—that metal–sulfur binding implicated an unacknowledged specialized group instead of conventional cysteinate ligands, an issue placed beyond doubt by the crystal structure of a tungsten aldehyde

oxidoreductase in 1995.⁷ It is, therefore, a matter of some satisfaction to the inorganic chemist interested in dithiolenes that this ligand type should present itself in biology against a background of extensive investigations of synthetic molecules. Indeed, the discovery of the pyranopterindithiolate **1** has generated a new imperative in the investigation of molybdenum and tungsten dithiolenes. In the sections that follow, we describe leading developments in structural and functional analogue chemistry involving both elements.

3.1. Molybdenum

With molybdenum, meaningful site analogues and analogue reaction systems of the SO and DMSOR families (Figure 1) have been achieved, but not yet in the XnO family, which is not further considered.

3.1.1. Analogues of the Sulfite Oxidase Family Sites

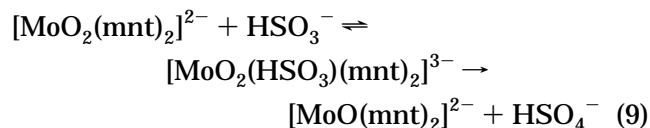
These site analogues require the preparation of monodithiolene species, an uncommon type of complex (excluding organometallic compounds). The problem has been approached by the two reaction sequences in Figure 10. Sequence 7 affords directly analogue **19** of site **4a** of oxidized SO and assimilatory nitrate reductase. The first step involves substitution of one silyloxy anion in $[\text{MoO}_2(\text{OSiPh}_3)_2]$ by bdt to give **18**, followed by replacement of the second anion by proton transfer from the hindered thiol to afford the desired analogue **19**.¹⁵⁹ Sequence 8 illustrates the preparation of two of six monodithiolene Mo^{V} complexes obtained in this work. Here the key step is formation of the monodithiolene complex **21** by removal of one bdt ligand from **20** with the strong electrophile PhSeCl. Chloride substitution

of **21** produces new complexes, including square pyramidal **22**, which approaches the proposed structure of the high-pH form of SO.

Complex **19** has a square pyramidal structure with the molybdenum atom displaced 0.74 Å from the OS₃ equatorial plane.¹⁵⁹ The equatorial oxo ligand has a trans influence of 0.06 Å on one Mo–S distance; the two other Mo–S distances are indistinguishable. Analysis of the positional deviations of the MoO₂S₃ coordination spheres of **19** and oxidized chicken liver SO determined at 1.9 Å resolution²¹ affords a weighted rms deviation of 0.26 Å. The Mo K-edge spectra and the EXAFS of the analogue and the enzyme are practically superimposable.¹⁶⁰ The collective evidence supports complex **19** as an accurate *structural* analogue of enzyme site **4a**. Current observations suggest that it is not sufficiently robust in solution to act as a functional analogue. While complex **19** most closely approaches the site, we have observed that **8** (Figure 2) shares the property of three anionic sulfur ligands in the equatorial plane. Also, the EPR spectrum of the monodithiolene complex [(Tp*)Mo^{VO}(bdt)] is reported to resemble that of the low-pH form of SO.¹⁶¹

Prior to crystallographic definition of the SO site, the bis(dithiolene) complexes [Mo^{IV}O(mnt)₂]²⁻, [Mo^{VO}Cl(mnt)₂]²⁻, and [Mo^{VI}O₂(mnt)₂]²⁻ were prepared as possible models of the active sites of SO.¹⁶² Like all [Mo^{IV,VO}L₄]^z species, [MoO(mnt)₂]²⁻ is square

pyramidal;¹³⁰ similarly, [Mo^{VI}O₂(mnt)₂]²⁻ adopts a highly distorted cis-octahedral structure¹⁶² always observed for [Mo^{VI}O₂L_{3,4}]^z complexes, several of which are shown in Figure 2. [Mo^{VI}O₂(mnt)₂]²⁻ was found to be cleanly reduced by bisulfite in acetonitrile containing a small amount of water according to reaction 9, which follows Michaelis–Menten kinetics with *K*_M = 0.010 M and *k*₂ = 0.87 s⁻¹ for the rate-determining step.¹⁶² Formulation of the intermediate is speculative.



The reaction was followed spectrophotometrically; product sulfate was verified by BaSO₄ precipitation. In a subsequent investigation in 1:1 acetonitrile/water (v/v), the same kinetics scheme was established with similar parameters (*K*_M = 0.039 M, *k*₂ = 1.02 s⁻¹).¹⁶³ Sulfite oxidation is inhibited by the structurally similar ions SO₄²⁻, H₂PO₄⁻, and H₂PO₃⁻, and the inhibition kinetics have been examined.¹⁶⁴ Reaction 9 is a specific expression of minimal reaction 2. Strictly speaking, it is not an analogue system because it utilizes bis(dithiolene) complexes. It is, however, a functional system which provides the

Table 2. Methods of Synthesis of Bis(dithiolene)Mo^{IV}O Complexes

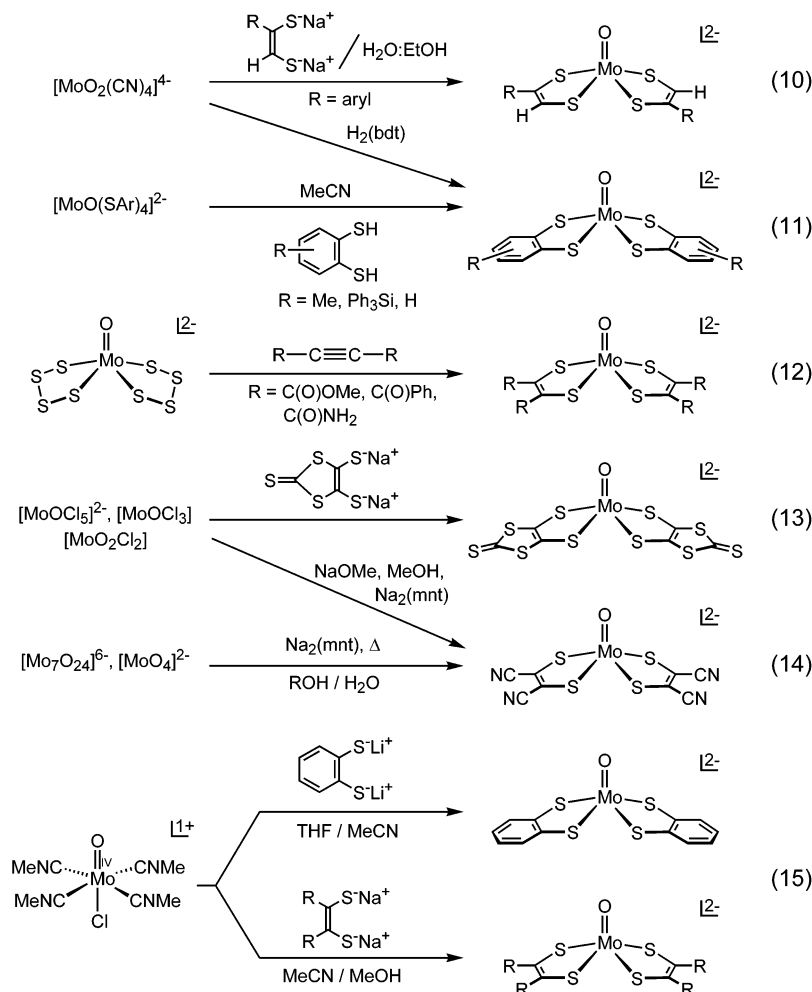


Table 3. Kinetics Data for Oxo-Transfer Reactions Mediated by Bis(dithiolene)molybdenum Complexes

complex	substrate	solvent	$k_2(298\text{ K})$ ($\text{M}^{-1}\text{ s}^{-1}$)	ΔH^\ddagger (kcal/mol)	ΔS^\ddagger (eu)	ref
$[\text{MoO}_2(\text{mnt})_2]^{2-}$	Et_3P	MeCN	0.109	15(1)	-13(5)	163
	Ph_3P	MeCN	0.0559	11(1)	-28(2)	163
	$(\text{MeO})_2\text{PhP}$	DMF	0.45	8.2(4)	-33(1)	147
	$(\text{MeO})_3\text{P}$	DMF	0.025	10(1)	-32(1)	147
$[\text{Mo}(\text{OPh})(\text{S}_2\text{C}_2\text{Me}_2)_2]^-$	Me_3NO	MeCN	2.0×10^2	8.1(6)	-21(2)	176
	$(\text{PhCH}_2)_3\text{NO}$	MeCN	16	9.5(1)	-21(1)	176
	$(\text{CH}_2)_4\text{SO}$	MeCN	1.5×10^{-4}	10.1(4)	-39(1)	179
	Me_2SO	MeCN	1.3×10^{-6}	14.8(5)	-36(1)	179
	$(\text{CH}_2)_4\text{SO}$	MeCN	5.2×10^{-3}	11.8(3)	-30(5)	176

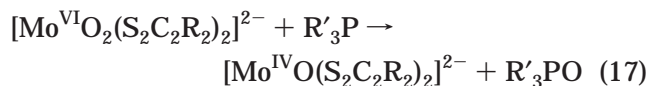
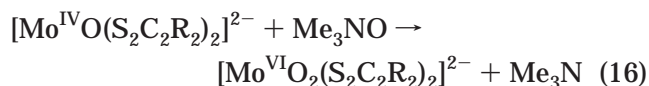
cleanest demonstration of the molybdenum-mediated oxidation of sulfite.

3.1.2. Analogues of the DMSO Reductase Family Sites

3.1.2.1. The $\text{Mo}^{\text{IV}}/\text{Mo}^{\text{VI}}\text{O}_2$ Reaction Couple.

Active sites in this family (5–7, Figure 1) require as analogues bis(dithiolene) complexes. Initial work that may be considered relevant to DMSOR systems utilized minimal reaction 2 in both directions with $[\text{MoO}(\text{S}_2\text{C}_2\text{R}_2)_2]^{2-}$ complexes as reactant or product. Principal routes to these complexes are summarized in Table 2. Reaction 10 involves cyanide substitution and concomitant elimination of water.^{127,153} In reaction 11, proton transfer from the dithiol leads to substitution of the monodentate arenethiolate ligands.^{127,165} Reaction 12 results in formation of dithiolene rings by suitably activated acetylenes and elimination of sulfur.^{166–168} Reaction 13 proceeds with chloride substitution and reduction of $\text{Mo}^{\text{V,VI}}$ by excess ligand.^{169,170} In reaction 14, oxo substitution by elimination of water in a protic medium and reduction of Mo^{VI} by ligand or an added reductant affords product.^{162,171} Reaction 15 involves substitution of isonitrile ligands by dianions and appears to be a general procedure.¹³⁰

With bis(dithiolene) $\text{Mo}^{\text{IV}}\text{O}$ complexes in hand, the corresponding $\text{Mo}^{\text{VI}}\text{O}_2$ species are accessible by oxo transfer, as illustrated in reaction 16 with the strong oxo donor trimethylamine *N*-oxide.^{165,172,173} The transformation is reversed by reaction 17 ($\text{R} = \text{CN}$; $\text{R}_3 = \text{Et}_3, \text{PhEt}_2, \text{Ph}_2\text{Et}, \text{Ph}_3$ ¹⁶³ and $(\text{MeO})_2\text{Ph}, (\text{MeO})_3$ ¹⁴⁷).



These reactions are not complicated by the comproportionation reaction 3, which is not observed, probably because of the negative charges of both complexes. Reduction of non-dithiolene $\text{Mo}^{\text{VI}}\text{O}_2$ complexes by tertiary phosphines is a common reaction. Its use in dithiolene systems is limited because few bis(dithiolene) $\text{Mo}^{\text{VI}}\text{O}_2$ species are sufficiently stable for isolation. $[\text{MoO}_2(\text{mnt})_2]^{2-}$ ¹⁶² and $[\text{MoO}_2(\text{bdt})_2]^{2-}$ ^{165,172} have been isolated as crystalline salts of known structure. Other species, such as $[\text{MoO}_2(\text{S}_2\text{C}_2(\text{CO}_2\text{Me})_2)_2]^{2-}$ and $[\text{MoO}_2(\text{S}_2\text{C}_2\text{Me}_2)_2]^{2-}$, have not been obtained in substance, presumably because of auto-redox reactions promoted by relatively electron-rich

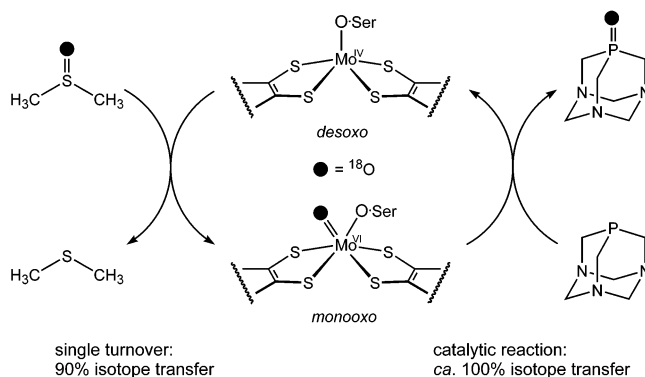
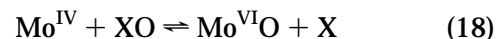


Figure 11. Double oxo-transfer reaction of *R. sphaeroides* DMSO reductase under single turnover or catalytic conditions using ^{18}O labeling. Note the essentially quantitative transfer of the label from Me_2SO to the phosphine.

ligands. Reactions 16 and 17 are examples of minimal reaction 2, i.e., of oxo transfer from and to substrate. Rate constants and activation parameters for reaction 17 are given in Table 3. Oxo transfer is second-order; saturation kinetics were not observed at high concentrations of tertiary phosphine. The substantial negative activation entropies are consistent with an associative transition state. Rate constants do not vary significantly with the cone angle of the phosphine. The range is restricted ($132\text{--}145^\circ$), and the results are consistent with attack by the phosphine on the oxo ligand rather than at the metal center.

3.1.2.2. The $\text{Mo}^{\text{IV}}/\text{Mo}^{\text{VI}}\text{O}$ Reaction Couple. The operation of this couple as minimal reaction 18 in DMSOR was demonstrated by the double-oxo-transfer reaction in Figure 11 with isotope labeling.¹⁷⁴ The



structure of the active site of *R. sphaeroides* DMSOR was not known at the time of the experiment, and the result was originally interpreted in terms of the $\text{Mo}^{\text{IV}}\text{O}/\text{Mo}^{\text{VI}}\text{O}_2$ reaction couple. That view is revised in Figure 11.

Synthesis. With the crystallographic structure determination of the foregoing enzyme²⁴ and other members of the DMSOR family, including trimethylamine *N*-oxide reductase (TMAOR),¹⁷⁵ it followed that any further meaningful development of analogue systems in terms of minimal reaction 18 must involve bis(dithiolene) desoxo Mo^{IV} and monooxo Mo^{VI} complexes. Synthetic access to these complexes, none of which was previously known, was accomplished by reactions 19 and 20 ($\text{R} = \text{Me}, \text{Ph}$; $\text{M} = \text{Mo}$ ^{156,176}).

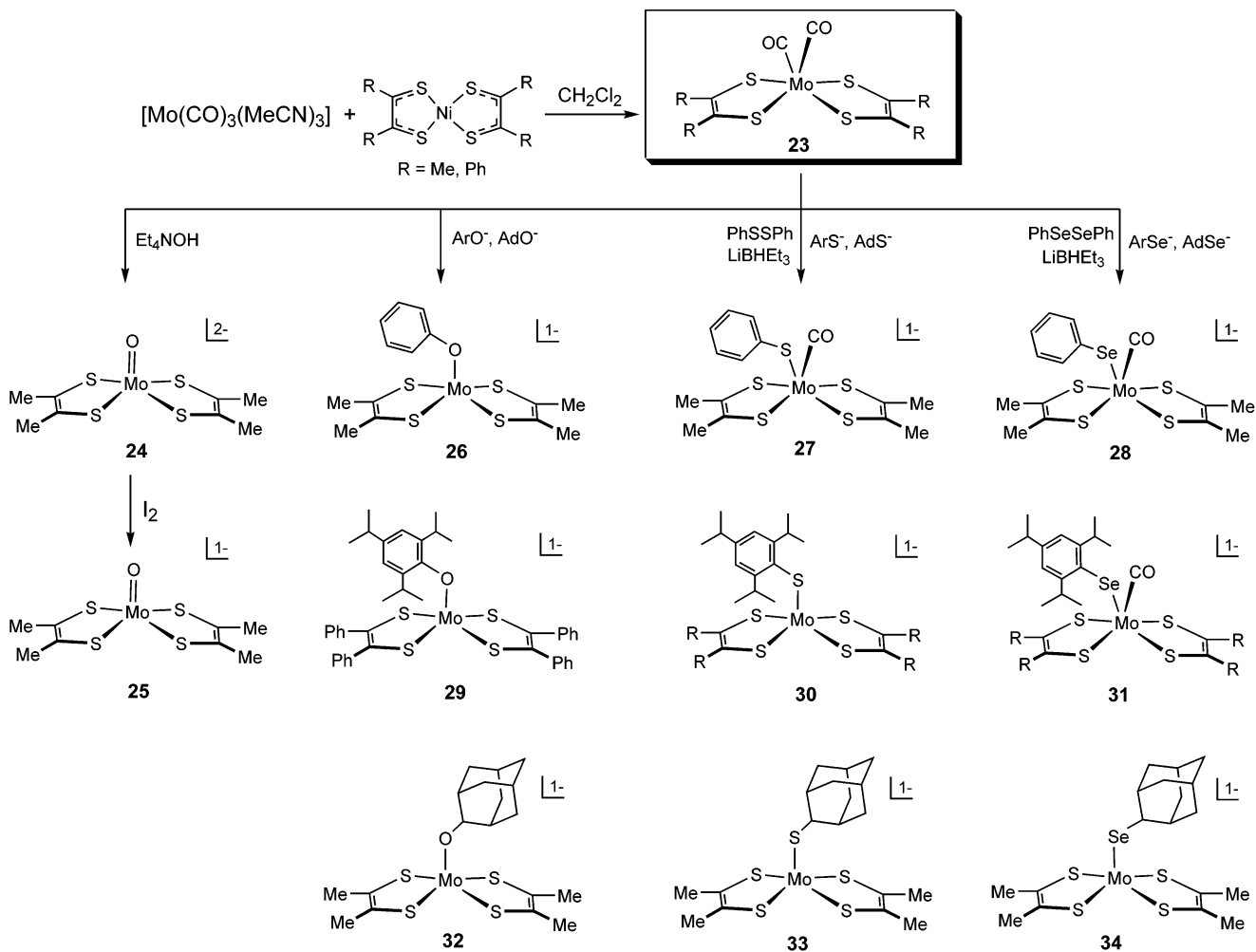
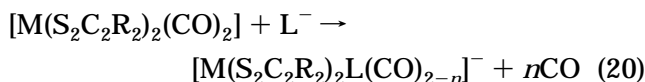
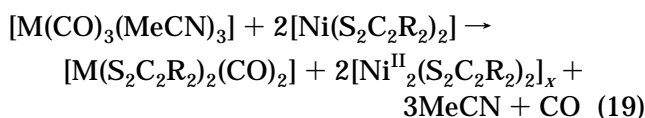


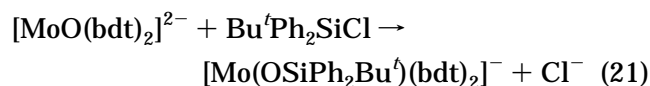
Figure 12. Synthetic pathways based on $[\text{Mo}(\text{S}_2\text{C}_2\text{R}_2)_2(\text{CO})_2]$ (**23**) leading to oxo (**24**, **25**), desoxo (**26**, **29**, **30**, **32–34**), and thiolate and selenolate monocarbonyl (**27**, **28**, **31**) bis(dithiolene) complexes.



The former reaction is an improvement over the original method of Schrauzer et al.,¹⁷⁷ which required photolysis of a mixture of $\text{M}(\text{CO})_6$ and $[\text{Ni}(\text{S}_2\text{C}_2\text{R}_2)_2]$. Reaction 19 can be interpreted as a four-electron oxidation of the metal by transfer of two dithione ligands from the nickel reactant. The product dicarbonyl **23** is a nonclassical molecule with possible oxidation state M^{II} or M^{IV} , and is part of the three-member electron-transfer series $[\text{M}(\text{S}_2\text{C}_2\text{R}_2)_2(\text{CO})_2]^{0,-,2-}$ which has been fully characterized.¹⁷⁸

The carbonyls in **23** are labile, and one or two are displaced in reaction 20. The synthetic scheme for molybdenum complexes is set out in Figure 12. All complexes are products of reaction 20. Reaction with hydroxide yields **24**, which cannot be obtained by the methods of Table 2, owing to the unavailability of the ligand in the free or noncomplexed form. This complex is readily oxidized to **25**. Anionic oxygen ligands displace both CO groups to give **26**, **29**, and **32**.

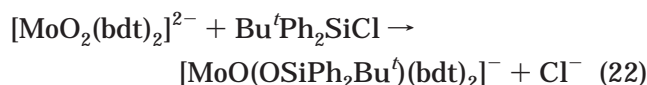
Hindered thiolates form **30** and **33** as opposed to the monocarbonyl **27** when benzenethiolate is used. Arylselenolates produce monocarbonyls **28** and **31**, reflecting the behavior found with molybdenum and tungsten that displacement of both carbonyls does not proceed, presumably because the longer M–Se bond lengths lead to less steric interaction of the ligand with the carbonyl. These complexes simulate the protein ligation of reduced sites **5b**, **6b**, and **7b**. Excluding the oxo and monocarbonyl species, the complexes are models of desoxo Mo^{IV} sites. Included is the aesthetically pleasing set of structural analogues **32–34** obtained with the sterically demanding 2-adamantyl group.¹⁷⁶ In earlier experiments, first-generation desoxo complexes had been obtained by silylation reactions such as 21.¹³⁰ All complexes



$[\text{Mo}(\text{S}_2\text{C}_2\text{R}_2)_2\text{L}]^-$ are square pyramidal with normal metric parameters, molybdenum atoms displaced ca. 0.7–0.8 Å above the S_4 plane toward the axial ligands, and dihedral angles between MoS_2 planes near 130°.

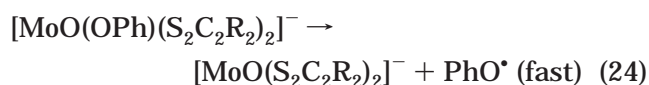
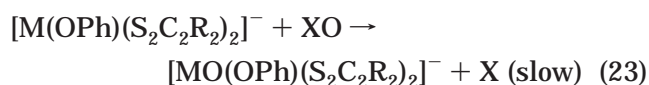
While desoxo Mo^{IV} complexes are now readily accessible, analogues of monooxo sites **6a** and **7a** are

not. Reaction 22 affords a monooxo product, which has an irregular cis-octahedral structure and is extremely sensitive to traces of water.¹³⁰ $[\text{Mo}(\text{OSiPh}_2\text{Bu}^t)_2]^{2-}$



$\text{Bu}^t(\text{bdt})_2]^-$ does not sustain clean oxo-transfer reactions, probably because of steric bulk of the axial ligand. The behavior of $[\text{MoO}(\text{OSiPh}_2\text{Bu}^t)(\text{bdt})_2]^-$ was also not promising. For example, no reaction was observed with 50 equiv of $(\text{CH}_2)_4\text{S}$ at 50 °C for 5 h. The complex was reducible with Ph_3P but with apparent byproduct formation. Steric effects and intrinsic instability are likely responsible for the lack of clean reactivity. Reaction of $[\text{Mo}(\text{OPh})(\text{S}_2\text{C}_2\text{Me}_2)_2]^-$ (**26**) with *N*-oxides or *S*-oxides forms $[\text{MoO}(\text{OPh})(\text{S}_2\text{C}_2\text{Me}_2)_2]^-$, which can be detected in solution but is too unstable to be isolated.¹⁷⁶ The majority of synthetic reactions in Figure 12 also apply to tungsten (*vide infra*). One conspicuous difference is the stability of W^{VI} complexes. Salts of both $[\text{WO}(\text{OPh})(\text{S}_2\text{C}_2\text{Me}_2)_2]^-$ ^{179,180} and $[\text{WO}_2(\text{S}_2\text{C}_2\text{Me}_2)_2]^{2-}$ ¹⁸¹ have been isolated and structurally characterized.

Oxo Transfer. Examination of a series of complexes $[\text{Mo}(\text{OR}')(\text{S}_2\text{C}_2\text{R}_2)_2]^-$ led to the selection of phenoxide complex **26** and its $\text{R} = \text{Ph}$ variant as suitably stable yet reactive analogues of reduced DMSOR site **5b**. Complexes such as **29** and **32** with large axial substituents react more slowly. The majority of kinetics data were collected with **26**. This species undergoes oxo-transfer reaction 23 ($\text{M} = \text{Mo}$) with $\text{XO} = \text{R}_3\text{NO}$ and R_2SO .^{176,179} Reactions are clean but slow; direct oxo transfer has been proven by isotope labeling with $\text{Ph}_2\text{Se}^{180}$ as the substrate. The systems are complicated by the autoredox follow-up reaction 24, whose occurrence is consistent with the observed formation of $[\text{MoO}(\text{S}_2\text{C}_2\text{R}_2)_2]^-$ and phenol. The reactions follow rate laws 25 ($\text{M} = \text{Mo}$) and 26.



$$-d[\text{M}^{\text{IV}}]/dt = k_2[\text{M}^{\text{IV}}][\text{XO}] \quad (25)$$

$$-d[\text{Mo}^{\text{VI}}\text{O}]/dt = k_1[\text{Mo}^{\text{VI}}\text{O}] \quad (26)$$

Representative kinetics data are provided in Table 3. The large negative activation entropies indicate an associative transition state. Second-order kinetics, associative transition states, and significant enthalpies of activation are found as well in non-dithiolene molybdenum-mediated oxo transfer.^{4,33,34,60,62,78} The proposed sequence of events in coupled reactions 23 and 24 is depicted in Figure 13. The rate constant for $(\text{CH}_2)_4\text{SO}$ (TMSO) reduction is ca. 100 times larger than that for Me_2SO , presumably because of reduced steric hindrance in binding to the molybdenum atom. The rate constant for Me_3NO vs Me_2SO ,

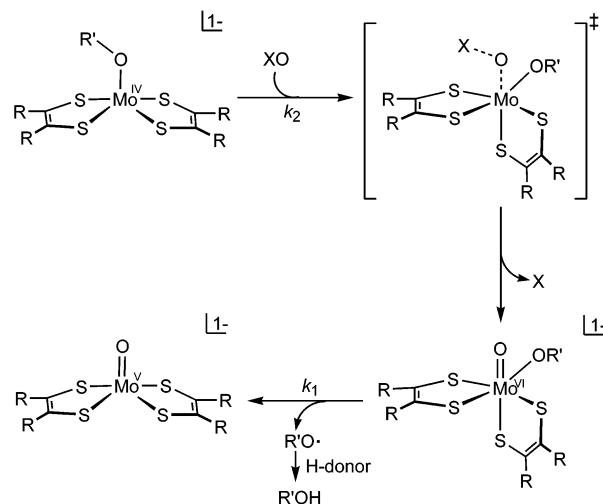


Figure 13. Summary of the oxo-transfer analogue reaction systems based on $[\text{Mo}^{\text{IV}}(\text{OR}')(\text{S}_2\text{C}_2\text{R}_2)_2]^-$ ($\text{XO} = \text{N-oxide, S-oxide}$), including the conversion of the $\text{Mo}^{\text{VI}}\text{O}$ intermediate to the Mo^{VO} final product.

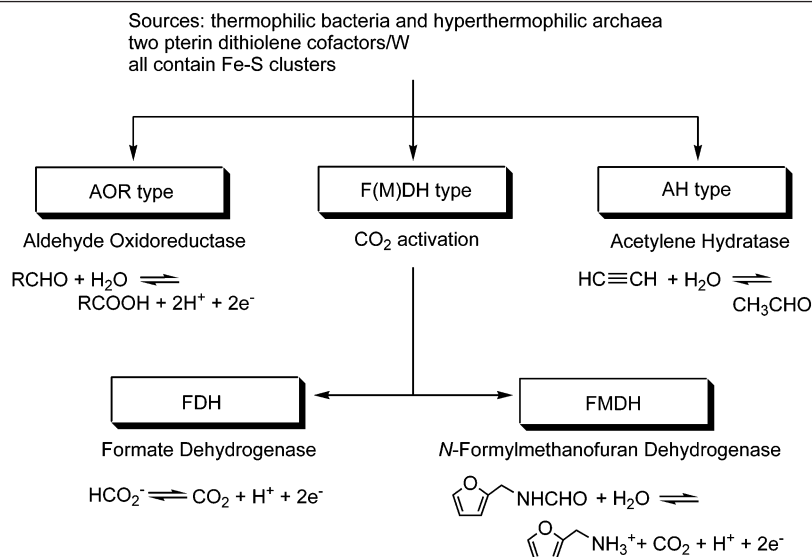
both biological substrates, is ca. 10^8 larger. While bond dissociation energies are not likely to be the only relevant factor, the rate constants follow the expected order Me_3NO (61 kcal/mol)¹⁸² > Me_2SO (87 kcal/mol).⁶¹ The nature of the transition state, as deduced from the corresponding tungsten analogue reaction systems, as well as the relevance of reaction 23 to enzymes, will be considered in a following section.

3.2. Tungsten

The discovery of tungstoenzymes in thermophilic bacteria and hyperthermophilic archaea^{141,183} is one of the most fascinating developments in contemporary bioinorganic chemistry. Because of the existence of such enzymes and of *Mo/W isoenzymes*,¹⁸⁴ molybdenum and tungsten dithiolene chemistry, insofar as possible, has been developed in parallel in the Harvard laboratory.

3.2.1. Tungstoenzymes

Summarized in Table 4 are the types of tungstoenzymes and the reactions catalyzed by them. The organization into types or families follows that put forward by Johnson et al.¹⁴¹ The three main families are recognized. Members of the AOR and F(M)DH families catalyze redox reactions. In contrast, AH catalyzes the hydration of acetylene. The enzyme from *P. acetylenicus* contains one tungsten center and one Fe_4S_4 cluster per molecule.¹⁸⁵ It should be noted that the protein-bound clusters $[\text{Fe}_4\text{S}_4(\text{S}\cdot\text{Cys})_3(\text{OH}/\text{OH}_2)]$ can effect hydration of *olefins*, as with aconitase.¹⁸⁶ Crystal structures of two enzymes in the AOR family, *P. furiosus* AOR⁷ and formaldehyde oxidoreductase,¹⁸⁷ have been determined. The active sites of these and other tungstoenzymes for which there is compositional information contain two pyranopterindithiolates per metal atom. Additional ligands in the first two enzymes are not well-defined but do not appear to derive from the protein backbone. It has been suggested that the oxidized site contains the grouping $\text{W}^{\text{VI}}\text{O}(\text{OH})$.³ *D. gigas* FDH is reported

Table 4. Types of Tungstoenzymes and Reactions Catalyzed

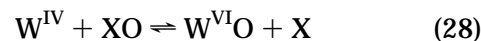
to bind one selenocysteinate and one hydroxyl or sulfide ligand.^{188,189} W-DMSOR is an isoenzyme of *R. capsulatus* Mo-DMSOR, obtained when the organism was cultured in a medium containing a much higher concentration of tungstate than molybdate. Its active site structure appears to resemble that of Mo-DMSOR, which, after some initial uncertainty, seems to be similar to that in *R. sphaeroides* DMSOR (5a, Figure 1). Isoenzymes of *E. coli* TMAOR are known, and their relative reactivities have been examined.¹⁹⁰

The properties of molybdenum and tungsten isoenzymes have been summarized elsewhere.^{32,180,184} Those of the DMSOR and TMAOR types do not readily fit into the classification scheme of Table 4, and may be viewed as “unnatural” in the sense that their formation was impelled by tungsten-biased growth media. As will be seen, these enzymes serve an interesting function by providing information about relative reactivities, a behavior that can be incisively assessed in analogue systems. It is against this background of tungsten enzymes and isoenzymes that structural and reactivity analogues have been pursued with bis(dithiolene) systems.

3.2.2. Analogue Systems

In general terms, tungsten-mediated oxo transfer and related synthetic chemistry are far less developed than for molybdenum. Summaries are available of leading results on oxo transfer through 1997,^{4,147} about the time interest in the subject increased markedly as tungstoenzymes assumed a more visible position. Relevant dithiolene chemistry began in 1992, with the preparation of $[\text{WO}(\text{mnt})_2]^{2-}$ ¹⁹¹ and the set $[\text{WO}(\text{bdt})_2]^{2-}$ and $[\text{WO}_2(\text{bdt})_2]^{2-}$.¹⁹² In 1996, $[\text{WO}_2(\text{mnt})_2]^{2-}$ was reported,¹⁹³ as were the naphthalene-2,3-dithiolate complexes $[\text{WO}(\text{ndt})_2]^{2-}$ and $[\text{WO}_2(\text{ndt})_2]^{2-}$.¹⁹⁴ The mnt complexes and $[\text{WO}(\text{bdt})_2]^{2-}$ were prepared by methods related to reactions 14 and 11, respectively, in Table 2. Two years later, a series of $[\text{WO}(\text{S}_2\text{C}_2\text{R}_2)_2]^{2-}$ complexes was prepared using a method related to reaction 10.¹⁵⁴ All tungsten complexes are isostructural and isoelectronic with their

molybdenum counterparts. Results for minimal reactions 27 and 28 are summarized in the following sections.



3.2.2.1. The $\text{W}^{\text{IV}}\text{O}/\text{W}^{\text{VI}}\text{O}_2$ Reaction Couple. Examples of reaction 27 in both directions have been documented as reactions 29–31. Substrate is reduced in reaction 29, which is the preparative method for $[\text{WO}_2(\text{bdt})_2]^{2-}$ and $[\text{WO}_2(\text{S}_2\text{C}_2\text{Me}_2)_2]^{2-}$.^{179,181,192} Reaction 30 produces the substrate of FDH enzymes; few details were reported.¹⁹¹ Substrate oxidation reactions 31 ($n = 0, 1$) are very slow and show second-order kinetics.¹⁴⁷ Rates of these reactions and reaction 17 are compared in a later section. Comproportionation reaction 3 is not observed. $[\text{WO}_2(\text{mnt})_2]^{2-}$ is also reduced by dithionite, H_2S , and thiols in reactions that apparently involve intermediate complexes with substrates.¹⁹³ Reaction of $[\text{WO}(\text{mnt})_2]^{2-}$ with elemental sulfur yields $[\text{WO}(\text{S}_2)(\text{mnt})_2]^{2-}$, containing the well-precedented side-on bound persulfide group located in the approximate position of an oxo ligand in $[\text{WO}_2(\text{mnt})_2]^{2-}$. This complex undergoes sulfur abstraction in reaction 32; addition of 1 equiv of phosphine leads to 50% formation of the $\text{W}^{\text{IV}}\text{O}$ product. Reaction kinetics were analyzed as a single-step second-order process.¹⁹³ Kinetics data for reactions 31 and 32 are given in Table 5. $[\text{WO}(\text{S}_2)(\text{mnt})_2]^{2-}$ displays some reactivity toward aldehydes accompanied by the formation of $[\text{WO}(\text{mnt})_2]^{2-}$;¹⁹³ however, the course of the reactions and the nature of the organic products are unclear. At this point, it is not known if persulfide is a physiological ligand. The $\text{W}^{\text{IV}}\text{O}/\text{W}^{\text{VI}}\text{O}_2$ reaction couple itself is unestablished in enzymes.

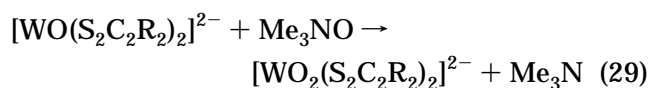
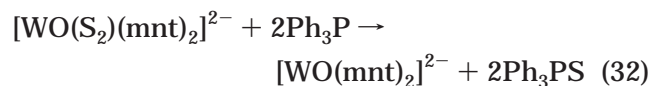
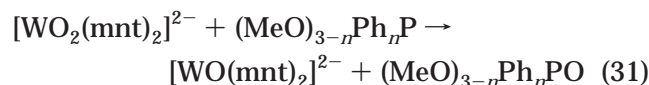
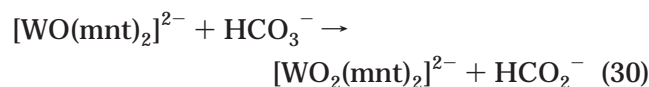


Table 5. Kinetics Data for Oxo-Transfer Reactions Mediated by Bis(dithiolene)tungsten Complexes

complex	substrate	solvent	$k_{2(298\text{ K})}$ ($\text{M}^{-1}\text{s}^{-1}$)	ΔH^\ddagger (kcal/mol)	ΔS^\ddagger (eu)	ref
$[\text{WO}_2(\text{mnt})_2]^{2-}$	Ph_3P	DMF	4.5×10^{-4}	11(1)	-33(1)	147
	$(\text{MeO})_3\text{P}$	DMF	9.7×10^{-6}	14(1)	-33(2)	147
$[\text{WO}(\text{S}_2)(\text{mnt})_2]^{2-}$	Ph_3P	MeCN	4.30	5.1(5)	-38(2)	193
	$(\text{CH}_2)_4\text{SO}$	MeCN	9.0×10^{-4}	11.6(4)	-33(1)	179
$[\text{W}(\text{OPh})(\text{S}_2\text{C}_2\text{Me}_2)_2]^-$	Me_2SO	MeCN	3.9×10^{-5}	14.4(2)	-30(1)	179
	Ph_3AsO	MeCN	3.2(1)	9.4(5)	-24(2)	180
	$\text{C}_5\text{H}_5\text{NO}$	MeCN	0.34	9.9(9)	-27(4)	180
	$(\text{CH}_2)_4\text{SO}$	MeCN	3.5×10^{-2}	10.8(1)	-29(1)	180
$[\text{W}(\text{OR}^2)(\text{S}_2\text{C}_2\text{Me}_2)_2]^-$ ^b	$(\text{CH}_2)_4\text{SO}$	MeCN	3.8×10^{-4}	15(1)	-24(4)	180
$[\text{W}(\text{OPh})(\text{S}_2\text{C}_2\text{Ph}_2)_2]^-$	$(\text{CH}_2)_4\text{SO}$	MeCN	3.0×10^{-3}	9.0(4)	-40(8)	152
$[\text{W}(\text{OPh})(\text{S}_2\text{C}_2\text{R}_2)_2]^-$ ^c	$(\text{CH}_2)_4\text{SO}$	MeCN	1.4×10^{-2}	8.6(7)	-38(5)	152
$[\text{W}(\text{OPh})(\text{S}_2\text{C}_2\text{R}'_2)_2]^-$ ^d	$(\text{CH}_2)_4\text{SO}$	MeCN	2.1×10^{-3}	10.9(1)	-34(4)	152
$[\text{W}(\text{OPr}^d)(\text{S}_2\text{C}_2\text{Me}_2)_2]^-$	Me_3NO	MeCN	0.93(5)	12(5)	-19(3)	180
	NMMO	MeCN	0.71	11(6)	-23(5)	180

^a $\text{R}^1 = \text{C}_6\text{H}_4\text{-}p\text{-CN}$. ^b $\text{R}^2 = \text{C}_6\text{H}_4\text{-}p\text{-NH}_2$. ^c $\text{R} = \text{C}_6\text{H}_4\text{-}p\text{-Br}$. ^d $\text{R}' = \text{C}_6\text{H}_4\text{-}p\text{-OMe}$.

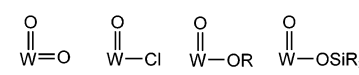
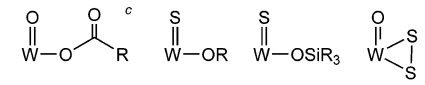
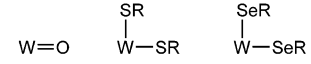
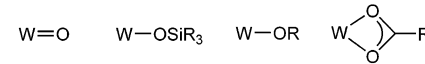
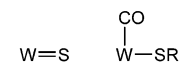
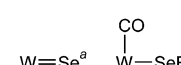
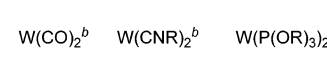


3.2.2.2. The $\text{W}^{\text{IV}}/\text{W}^{\text{VI}}\text{O}$ Reaction Couple. Minimal reaction 28 with dithiolene complexes was unexplored prior to the recent emergence of tungsto-enzymes. Because of the relative stability of $\text{W}^{\text{VI}}\text{O}$ complexes, analogue reaction systems have proven more amenable to investigation than those involving $\text{Mo}^{\text{VI}}\text{O}$ species.

Synthesis. Substantial effort has been investigated in exploratory synthesis in order to establish stable ligation modes in bis(dithiolene) complexes. A second phase of synthesis began in 1998, with the preparation of a wide variety of bdt complexes.¹¹ These includes several desoxo and monooxo complexes $[\text{W}(\text{OSiR}_3)(\text{bdt})_2]^-$ and $[\text{WO}(\text{OSiR}_3)(\text{bdt})_2]^-$, respectively, obtained by reactions analogous to 21 and 22. Also synthesized were $[\text{WOCl}(\text{bdt})_2]^-$, from $[\text{WO}(\text{OSiR}_3)(\text{bdt})_2]^-$ and Me_3SiCl , and the monosulfido complex $[\text{WS}(\text{OSiR}_3)(\text{bdt})_2]^-$, most readily obtained from $[\text{W}(\text{OSiR}_3)(\text{bdt})_2]^-$ and $(\text{PhCH}_2\text{S})_2\text{S}$. Like their molybdenum counterparts, these are first-generation site analogues.

To approach more closely the coordination environment in enzymes, the reaction scheme in Figure 14 has been implemented. It is based on reactions 19 and 20 ($\text{R} = \text{Me}, \text{Ph}$; $\text{M} = \text{W}^{152,155,179-181,195}$), some of which are parallel to reactions in the molybdenum scheme of Figure 12. The key compound is the dicarbonyl **35**, which can be converted to monooxo (**36**, **37**, **41**), dioxo (**38**), desoxo (**39,40**), monosulfido (**42**), and thiolate and selenolate monocarbonyl (**43**, **44**) complexes. Five-coordinate thiolate and selenolate complexes are presently unknown. Reactions of **35** with the strongly hindered ligands AdQ^- or 2,4,6- $\text{Pr}^i_3\text{C}_6\text{H}_2\text{Q}^-$ ($\text{Q} = \text{S}, \text{Se}$) in excess afford stable monocarbonyl complexes.^{181,195} Figure 14 provides a partial accounting of the bis(dithiolene) complexes

Table 6. Functional Groups in Mononuclear Bis(dithiolene)tungsten(IV,V,VI) Complexes

Ox. State	Group	Refs
W^{VI}		11, 179, 180, 192-194
		11, 193
W^{V}		11, 155, 195
W^{IV}		11, 154, 155, 180, 195
		155, 195
		155, 195
		11, 155, 178

^a Not proven by a structure determination. ^b Ambiguous oxidation state. ^c Jiang, J.; Holm, R. H., submitted for publication.

that have been prepared. The full inventory is contained in Table 6, which lists complexes in terms of their non-dithiolene ligands. Among the additional entries are terminal sulfide and selenide,^{155,181} $\eta^{1,2}$ -carboxylate,¹⁸¹ bis(thiolate) and bis(selenolate)¹⁸¹, and the η^2 -persulfide species¹⁹³ encountered earlier. It remains to be learned which of these ligation modes are physiologically relevant. However, contained within this extensive set are the desoxo W^{IV} and monooxo W^{VI} required for examination of reaction 28.

Oxo Transfer. The reaction system $[\text{W}(\text{OSiPh}_2\text{Bu}^t)(\text{bdt})_2]^-/\text{XO}$ in acetonitrile provided the initial examples of the $\text{W}^{\text{IV}}/\text{W}^{\text{VI}}\text{O}$ reaction couple.¹¹ Substrates $\text{XO} = N$ -oxides, S -oxides, Ph_2SeO , Ph_3PO , and $\text{Ph}_3\text{-AsO}$, often present in large excess in systems at 60 °C for ≥ 15 h, are reduced. Except for Me_3NO and N -morpholine- N -oxide, reactions are sluggish and incomplete. In particular, Me_2SO and $(\text{CH}_2)_4\text{SO}$ were

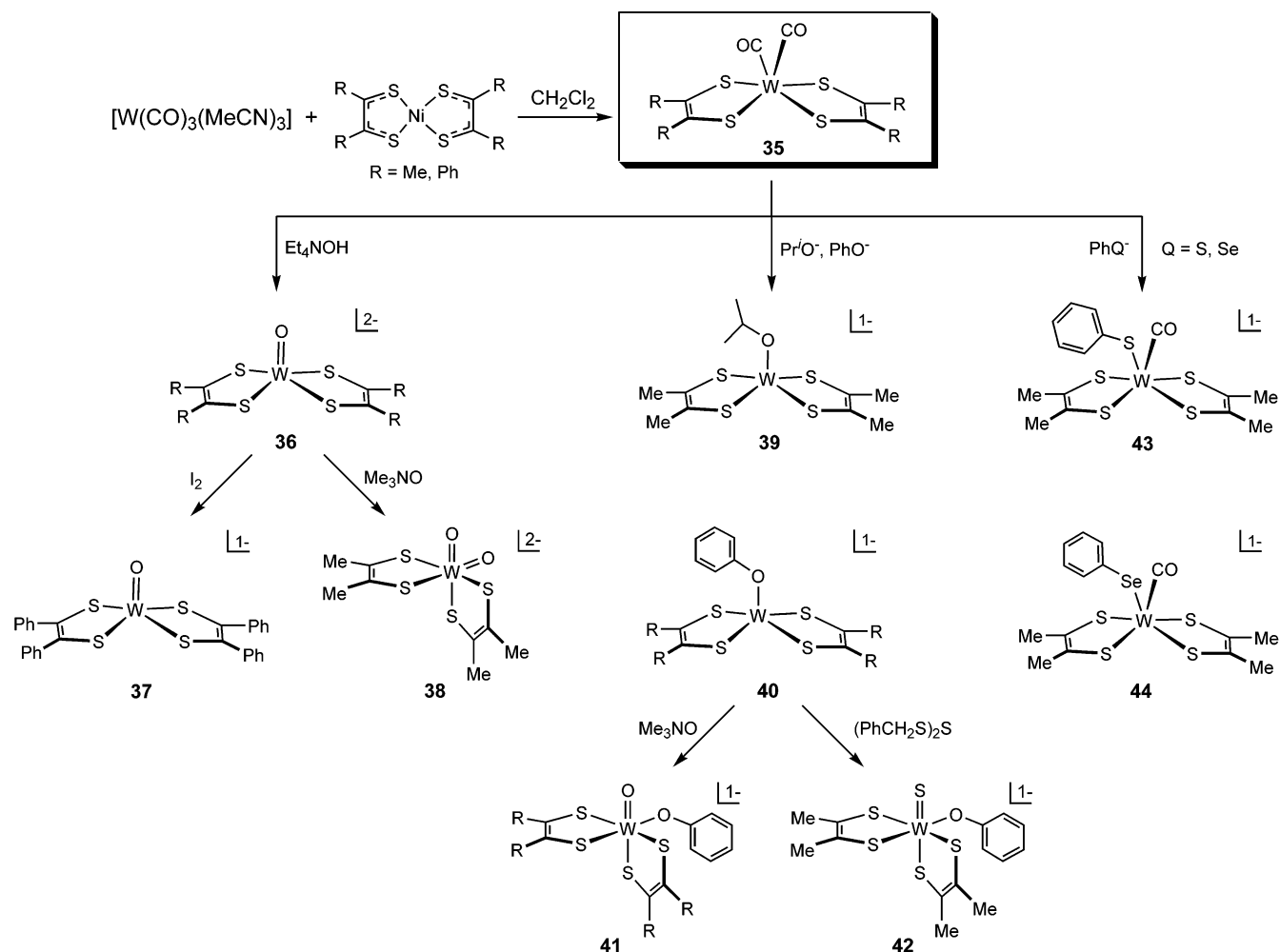


Figure 14. Synthetic pathways based on $[W(S_2C_2R_2)_2(CO)_2]$ (**35**) leading to monooxo (**36**, **37**, **41**), dioxo (**38**), desoxo (**39**, **40**), monosulfido (**42**), and thiolate and selenolate monocarbonyl (**43**, **44**) bis(dithiolene) complexes.

only partially reduced under these conditions. Slow reaction rates, especially for the *S*-oxides, presumably arise in large part from the bulky silyloxy axial ligand. However, it is clear that with the same substrate the tungsten system is far more active than the molybdenum system in substrate reduction, a behavior found to be general (vide infra).

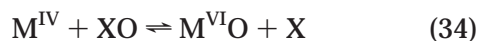
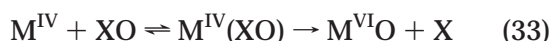
Reaction 23 (R = Me, Ph; M = W) represents well-behaved oxo-transfer systems which are conveniently monitored spectrophotometrically.^{152,180} Like their molybdenum analogues, the complexes $[W(OPh)(S_2C_2R_2)_2]^-$ (**40**) are readily accessible. Product complexes $[WO(OPh)(S_2C_2R_2)_2]^-$ (**41**) have been independently prepared. While they are extremely sensitive to dioxygen and water, they do not exhibit the tungsten counterpart of reaction 24, thereby simplifying the kinetics analysis. With $XO = N$ -oxides, *S*-oxides, and Ph_3AsO , reactions proceed to completion. Direct oxo transfer was proven with use of $Ph_2Se^{18}O$. When the axial ligand is changed to isopropoxide, the reactivity is diminished. The reaction of $[W(OPr^i)(S_2C_2Me_2)_2]^-$ (**39**) in neat $(CH_2)_4SO$ is ca. 200 times slower than the reaction of **40** with the same substrate, allowing spectrophotometric rate measurements with the more reactive *N*-oxide substrates. Kinetics data are summarized in Table 5. Second-order rate law 25 (M = W) is observed, and activation

entropies indicate an associative pathway. Hence, the kinetics behavior is the same as for molybdenum-mediated reaction 23 (Table 3), but the reactions are faster.

Tungsten-mediated reaction 23 is an analogue reaction system of W-DMSOR, and the $W^{VI}O$ product complex is a structural analogue of the active site of the oxidized enzyme. Molecule **41** (R = Me) exhibits an irregularly distorted octahedral structure with cis oxo and phenolate ligands.¹⁸⁰ This structure and that of *R. capsulatus* W-DMSOR, determined with data up to 2.0 Å,¹⁹⁶ have the common feature of cis oxygen ligands. The bond distances $W-O = 1.76$ and 1.89 Å and $W-S = 2.44$ Å from tungsten EXAFS correspond fairly closely with the crystallographic distances of **41** (1.728, 1.994, and 2.43 Å (mean of 4)). When the two structures are superimposed, analysis of the positional deviations of the WO_2S_4 coordination spheres leads to a weighted rms deviation of 0.39 Å. While it is difficult to be exact about the structural differences at this stage of resolution of the protein structure, it is evident that the synthetic complex and the protein site have a similar overall stereochemistry and bond lengths. This is currently the only meaningful comparison that can be made between a synthetic complex and the complete coordination sphere of a tungstoenzyme site.

3.3. Mechanistic Aspects of Oxo Transfer

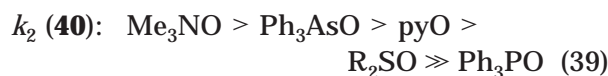
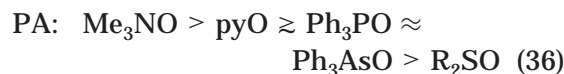
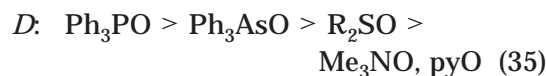
The distinction most likely to be required in interpreting oxo-transfer reaction pathways is between saturation and nonsaturation kinetics, i.e., between reactions 33 and 34.



In the former,⁵ a pre-equilibrium substrate binding reaction is followed by oxo transfer in a rate-determining first-order reaction; at sufficient [XO], the rate is independent of [XO]. In the latter, the reaction is first-order in both reactants, and no pre-equilibrium binding influences the kinetics. A few cases of apparent saturation kinetics have been found with non-dithiolene complexes,^{5,197–200} and one example, reaction 9, has been found with a bis(dithiolene) Mo^{IV}O/Mo^{VI}O₂ couple. In either pathway, a principal issue is the nature of the intermediate or transition state. There is no experimental information bearing on this matter for reactions of type 33. However, Thapper et al.²⁰¹ have examined possible intermediates in the sulfite oxidase analogue reaction 9 by a combination of extended Hückel and DFT calculations. Intermediates were considered arising from direct attack of HSO₃[−] on the molybdenum center to produce a seven-coordinate intermediate or on one of the terminal oxo groups in a six-coordinate intermediate. In both cases, the attack is by the lone pair of electrons on the sulfur atom. The calculations indicate a six-coordinate intermediate formed over a barrier of ca. 22 kcal/mol above ground-state [MoO₂(mnt)₂]^{2−}. The alternate pathway was higher in energy by 12 kcal/mol. On this basis, the intermediate in reaction 9 might be more specifically described as [MoO(OSO₃H)(mnt)₂]^{3−}. The proposal of substrate attack at an oxo group was offered earlier for sulfite oxidase² and for reaction 9.¹⁶³ It finds substantial precedence in proposals for the mechanism of oxo transfer from Mo^{VI}O₂ groups to tertiary phosphines^{4,202} and in theoretical calculations on non-dithiolene systems.^{63,66} This is the likely pathway for oxidation of phosphorus substrates in Tables 3 and 5.

Reactions of general type 34 are more common than 33. The operation of this pathway for bis(dithiolene) complexes of molybdenum and tungsten, with attendant second-order rate constants and negative activation entropies, is documented by the data in Tables 3 and 5. Hereafter, we consider substrate *reductions* which serve as analogue reaction systems for DMSOR and TMAOR. It should be noted that, for the most part, enthalpic and entropic contributions to activation free energies are comparable. Thus, for the prototypic reaction systems [M(OPh)(S₂C₂Me₂)₂]/(CH₂)₄SO, $T|\Delta S^\ddagger|$ is 53% (Mo) and 46% (W) of ΔG^\ddagger . Against a background of significant entropic contributions, mechanistic considerations reduce to identification of the enthalpic factors that control reaction rates. Rates are sensitive to substrate type, covering ranges of ca. 10⁸ and 10⁵ for molybdenum- and tungsten-mediated reactions. The distinction between the fast *N*-oxide and slow

S-oxide substrates is clearly evident. Relevant substrate properties—bond dissociation energies *D*, proton affinities PA, and solution basicity constants—fall in the order of series 35–37. Numerical values are given elsewhere.¹⁸⁰ These series may be compared to the experimental rate constant orders 38 and 39 for one Mo^{IV} (**26**) and two W^{IV} complexes (**39**, **40**). In series 39, Me₃NO is designated the fastest substrate because its reaction with **40** under the same conditions as Ph₃AsO was too fast to measure by the spectrophotometric technique used. No bis(dithiolene) molybdenum or tungsten complex was observed to reduce Ph₃PO, for which *D* = 133 kcal/mol.



The inverse of series 35 would be expected to apply to *k*₂ if substrate X–O bond weakening were the dominant feature of the transition state. However, Ph₃AsO reacts more rapidly than would be expected on this basis (Table 5). (The rate order Ph₃AsO > R₂SO is also found for reaction 4.⁶² The source of this order is unclear.) Series 36 or 37 is relevant if proton affinities in the gas or aqueous phase convey binding affinities toward M^{IV} centers. Series 38 and particularly 39 parallel this order, suggesting an early transition state with substantial M^{IV}⋯OX bond-making.

In an attempt to provide further information on the transition state involved in substrate reduction, the kinetics of reaction 40 in Figure 15 were determined at 298 K in acetonitrile.¹⁵² Here, the electron density at the tungsten atom can be modulated in a predictable way by variation of axial and equatorial substituents X' and X, respectively, in the essentially constant stereochemistry of reactants **45** and products **46**. A set of 25 complexes designated by the matrix [X₄X'] was examined. Relative to the reference complex [W(OPh)(S₂C₂Ph₂)₂][−], substituents are electron-withdrawing groups (EWGs) or electron-donating groups (EDGs). Linear free energy relationships (LFERs) between *E*_{1/2} values and the Hammett constant σ_p for the reversible electron-transfer series [Ni(S₂C₂(C₆H₄-*p*-X)₂)₂]^{0,−2−} and [W(CO)₂(S₂C₂(C₆H₄-*p*-X)₂)₂]^{0,−2−} demonstrate a substituent influence on electron density distribution at the metal center. The substituent effects are propagated through phenyl groups to the unsaturated chelate rings of the nickel and tungsten complexes to measurable extents which are manifested as LFERs.

The reactions 40 with constant (CH₂)₄SO substrate are second-order, with large negative activation

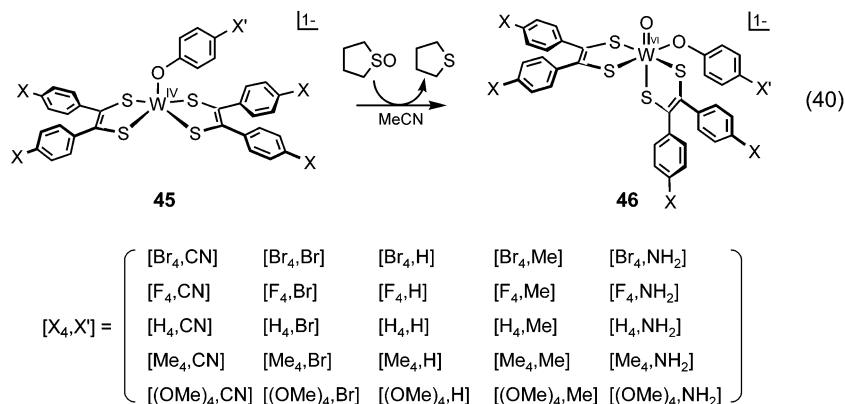


Figure 15. Depiction of generalized reaction 40 used to investigate the effects of electronic properties of W^{IV} complexes on the rates of reduction of the constant substrate $(\text{CH}_2)_4\text{SO}$. Substituents X (equatorial) and X' (axial) in the reactants **45** and the products **46** are shown in the matrix $[X_4, X']$, which describes 25 substituent combinations.

entropies indicative of an associative transition state (Table 5). Rate constants at 298 K adhere to the Hammett equations $\log(k^{[X_4, X']}/k^{[X_4, \text{H}]}) = \rho_{\text{ax}}\sigma_{\text{p}}$ and $\log(k^{[X_4, X']}/k^{[\text{H}_4, X']}) = 4\rho_{\text{eq}}\sigma_{\text{p}}$. EWGs and EDGs have opposite effects on rates such that $k^{\text{EWG}} > k^{\text{EDG}}$. The effect of X' on reactivity is found to be ca. 5 times greater than that of X ($\rho_{\text{a}} = 2.1$, $\rho_{\text{e}} = 0.44$) in the Hammett equation. EWRs increase redox potentials. This property is expected to extend to W^{IV} complexes, but it cannot be directly established because the complexes **45** do not, in general, support reversible redox reactions. The order $k^{\text{EWG}} > k^{\text{EDG}}$ is opposite to the expected ease of oxidation of W^{IV} , $E_{\text{EWG}} > E_{\text{EDG}}$. This lack of correlation between rate constant and oxidizability suggests that electron transfer, as it occurs with transfer of an oxygen atom to the metal center and accompanying oxidation to W^{VI} , is not dominant in the rate-determining step. A stepwise oxo-transfer reaction pathway is proposed in the form of the qualitative reaction coordinate in Figure 16.¹⁵² An early transition state T_1 , of primary $\text{W}^{\text{IV}}\text{--O}(\text{substrate})$ bond-making character, is rate-limiting. This is followed by a six-coordinate substrate complex **I** and a second transition state T_2 proposed to involve atom and electron transfer, leading to the development of the $\text{W}^{\text{VI}}\text{=O}$ group present in the products **46**. EWGs tend to make the W^{IV} center more electrophilic than do EDGs, promoting substrate binding and lowering ΔG^\ddagger_1 . In the limit of an infinitely strong EWG, intermediate **I** and T_2 are suppressed, and the situation devolves to a single transition state. In the proposed interpretation, the rate-limiting transition state is early. Its exact structure cannot be specified; the Hammond postulate presumably requires reduction of the dihedral angle of 128° between chelate rings in $[\text{W}(\text{OPh})(\text{S}_2\text{C}_2\text{Me}_2)_2]^-$ to ca. 100° found in $[\text{WO}(\text{OPh})(\text{S}_2\text{C}_2\text{Me}_2)_2]^-$.¹⁸⁰ A DFT analysis of the reaction system $[\text{M}(\text{OMe})(\text{S}_2\text{C}_2\text{Me}_2)_2]^-/\text{Me}_2\text{SO}$ has led to a transition state, based on theoretical $\text{M}\text{--}\text{OSMe}_2$ and $\text{O}\text{--}\text{S}$ bond lengths, that is biased toward the T_2 description.²⁰³ In this analysis and that for $[\text{MoO}_2\text{--}(\text{SCH}_2\text{CH}=\text{NH})_2]^-/\text{Me}_3\text{P}$,⁶⁶ a model for a real system,⁶² a single transition state is considered. The proposal for two transition states (Figure 16) has been made because of a lack of correlation between oxidizability of W^{IV} and rate constants. The kinetics work based on reactions 23^{176,180} and 40¹⁵² is the most detailed

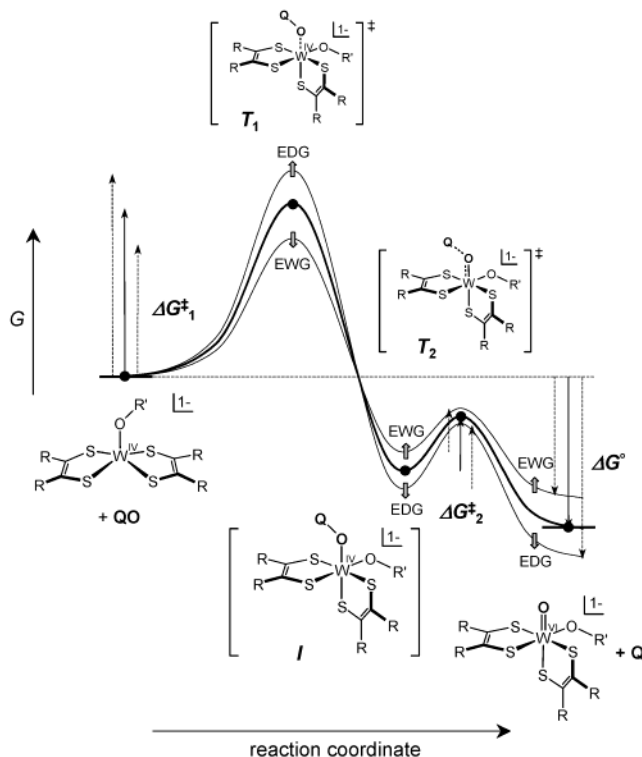


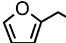
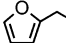
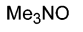
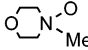
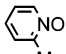
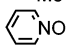
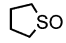
Figure 16. Proposed reaction coordinate for reaction 40 (Figure 15) with schematic representations of transition states (T_1 , T_2) and intermediate (**I**). The thick line refers to a system initially containing reference complex $[\text{W}(\text{OPh})(\text{S}_2\text{C}_2\text{Ph}_2)_2]^-$, and other lines refer to complexes $[\text{W}(\text{OR}')(\text{S}_2\text{C}_2\text{R}_2)_2]^-$ containing electron-donating groups (EDG) or electron-withdrawing groups (EWG) X/X' in the substituents $\text{R}' = p\text{-C}_6\text{H}_4\text{X}'$ and $\text{R} = p\text{-C}_6\text{H}_4\text{X}$.

mechanistic investigation of oxo transfer mediated by a biological metal.

3.4. Relative Reactivity of Molybdenum and Tungsten

The emergence of molybdenum and tungsten isoenzymes¹⁸⁴ and the recent synthesis of corresponding bis(dithiolene) complexes of these elements has permitted the first examination of relative reactivities in natural and synthetic systems. While the results are not yet extensive, they merit consideration at this stage. Collected in Table 7 are relative reactivi-

Table 7. Relative Reactivities of Molybdenum and Tungsten Isoenzymes

isoenzyme	reaction	W/Mo reactivity ratio	ref	
FMDH	 NHCHO + H ₂ O →	0.2 ^a	204-206	
	 NH ₃ ⁺ + CO ₂ + H ⁺ + 2e ⁻	0.3 ^b		
TMAOR	XO + 2H ⁺ + 2e ⁻ → X + H ₂ O ^c	XO		
			2.2	
			4.1	
			4.2	
			2.0	190
		Me ₂ SO	no reaction for Mo <i>k</i> _{cat} / <i>K</i> _M = 5.0 × 10 ⁴ M ⁻¹ s ⁻¹ for W	
		Ph ₂ SO	no reaction for Mo <i>k</i> _{cat} / <i>K</i> _M = 2.7 × 10 ⁴ M ⁻¹ s ⁻¹ for W	
	no reaction for Mo <i>k</i> _{cat} / <i>K</i> _M = 2.0 × 10 ⁶ M ⁻¹ s ⁻¹ for W			
DMSOR	Me ₂ SO + 2H ⁺ + 2e ⁻ ⇌ Me ₂ S + H ₂ O ^d	17 (forward reaction) 0.06 (backward reaction)	196	

^a *M. thermoautotrophicum*. ^b *M. wolfei*. ^c *E. coli*. ^d *R. capsulatus*.

Table 8. Relative Reactivities of Molybdenum and Tungsten Bis(dithiolene) Complexes in Oxo Transfer at 298 K

reaction	substrate	<i>k</i> ₂ ^W / <i>k</i> ₂ ^{Mo}	refs
M^{VI}O₂ → Mo^{IV}O			
(17) (R ₂ C ₂ S ₂ = mnt)	(MeO) ₂ PhP	0.001	147
	(MeO) ₃ P	0.0004	147
	(EtO) ₂ MeP	0.003	147
M^{IV}O → M^{VI}O₂			
(16) (R ₂ C ₂ S ₂ = bdt)	Me ₃ NO	2.5	192
M^{IV} → M^{VI}O			
(23) (R = Me)	Me ₂ SO	30	179, 180
(23) (R = Me)	(CH ₂) ₄ SO	6	179, 180
(23) (R = Ph)	(CH ₂) ₄ SO	8.8	176, 179

ties as ratios of rate constants for three isoenzymes.^{190,196,204–206} Structural information is available only for *R. capsulatus* Mo- and W-DMSOR, which have oxidized site **5a** (Figure 1). In the FMDH case, the reaction is substrate oxidation, possibly involving the M^{VI}O/M^{IV} couple. Here the molybdoenzyme is more reactive. *N*-Oxide substrates are reduced by TMAOR, but *S*-oxides are reported to be unreactive. With DMSOR, the indicated reaction has been examined in both directions. These enzymes utilize the M^{IV}/M^{VI}O reaction couple. Table 8 contains the small database of relative reactivities of bis(dithiolene) complexes in substrate oxidation and reduction reactions under the same experimental conditions. Comparison of relative reactivities of Mo/W isoenzymes and pairs of isostructural Mo/W complexes at strict parity of ligation reveals that *oxo transfer from substrate to metal* (M^{IV} → M^{VI}O) is faster with tungsten and that *to substrate from metal* (M^{VI}O → M^{IV}) is faster with molybdenum. These results demonstrate a *kinetic metal effect* on direct oxo transfer for the analogue complexes and for isoenzymes, provided the catalytic sites are isostructural. The effects are not large for *N*-oxide and *S*-oxide sub-

strates, but for reasons that are unclear, rate constants are orders of magnitude different for phosphorus substrate oxidation.

Factors that might influence the relative activation energies of transition states have been pointed out.¹⁴⁷ These include bond energies, although experimental data are sparse. For MOCl₄, *D*_{WO} - *D*_{MoO} ≈ 26–29 kcal/mol from thermochemical data and theoretical estimates. For strictly analogous redox couples, *E*_{W} < *E*_{Mo}, with the potential difference decreasing as bond covalency increases. There are no exceptions to this periodic property. In oxo transfer from substrate, both of these effects would favor more rapid reactions for the tungsten-mediated reaction if they contributed significantly to Δ*G*[‡]. While a corresponding study for molybdenum complexes has not been carried out, it seems intuitively reasonable that the reaction coordinate of Figure 16 would apply to molybdenum-mediated reactions. If so, the binding of the same substrate to Mo^{IV} is weaker than that to W^{IV}. The kinetic metal effect is quite small for substrate reduction, but it does imply a highly concerted transition state with X–O bond-weakening and W–O bond-making, with incipient atom transfer and metal oxidation. The proposed reaction pathway is attractive because of the substantial body of results that support it.¹⁵² As always, the best mechanism is that with the least evidence against it. Whether or not the observed kinetic metal effect is evidence against the proposed pathway remains to be seen. The matter of mechanism remains open. Further consideration of the nature of the transition state may be helped by theoretical studies of the molybdenum and (if possible) tungsten reaction coordinates, as has been done for the systems Mo^{VI}O₂/R₃P,^{63,66} Mo^{VI}O₂/HSO₃⁻,²⁰¹ and Mo^{IV}/Me₂SO/Me₃NO.^{203,207}}}}}

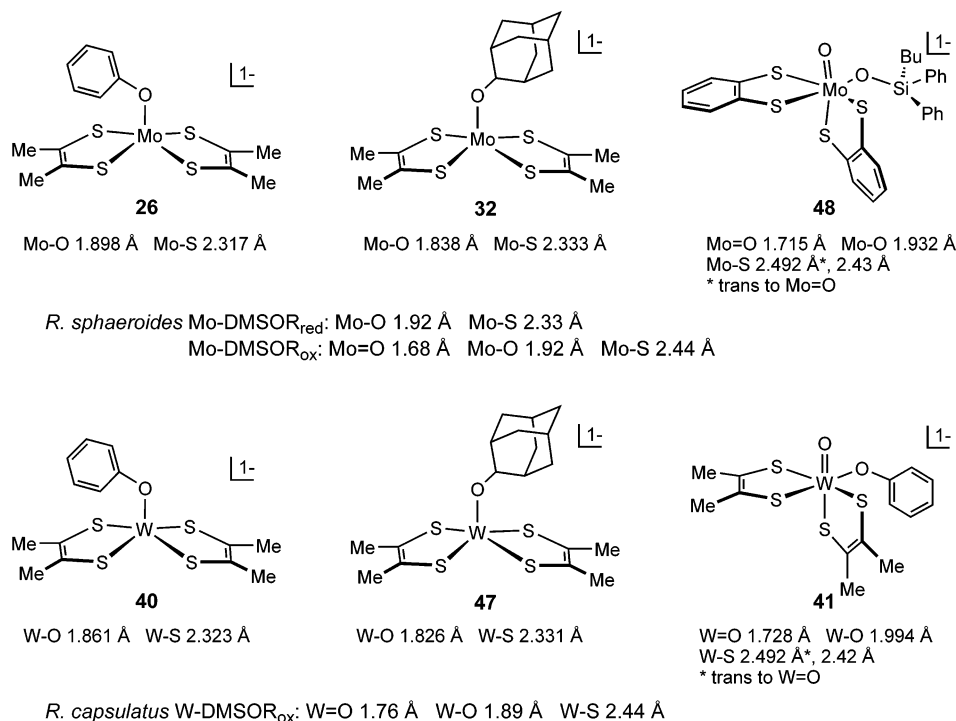


Figure 17. Comparison of bond distances between sites of DMSOR enzymes and analogues of those sites.

3.5. Relation to Enzymes

In research related to enzymes, the intention has been to disclose with accurate minimal active site representations intrinsic structural, electronic, and reactivity features, unmodified by protein structure and environment. In this way, the fundamental behavior of metal sites can be revealed. Meaningful synthetic analogues of a protein site must have the attributes of approaching or achieving the *structure* and *function* of that site.

3.5.1. Structure

Complexes synthesized prior to the proposal of an ene-1,2-dithiolate chelate ring in 1982,¹⁵⁸ or before crystallographic proof of that structural unit in 1995,⁷ could not be expected to be accurate structural models. Yet, as mentioned below, certain of these non-dithiolene complexes played a significant role in the development of function. With the preparation of molybdenum and tungsten bis(dithiolene) species starting in 1986,¹²⁷ more accurate analogues came into reach. The first group of complexes, of which $[M^{IV}O(bdt)_2]^{2-}$ and $[M^{VI}O_2(bdt)_2]^{2-}$ are representative, contain the indicated monooxo and dioxo groups, and support oxo-transfer reactions 2 and 27. They are possibly relevant to the site in *A. faecalis* arsenite oxidase,²⁰⁸ which is a molybdoenzyme with two pyranopterindithiolate and one or two oxo ligands, and no protein ligand. In the crystal form reported, the site has a square pyramidal unit with an apical oxo ligand, for which **24** (Figure 12) should be a good structural model. The protein structure is insufficiently accurate for a detailed comparison with synthetic complexes. Thereafter, a large array of bis(dithiolene) species was synthesized, primarily of the desoxo M^{IV} and monooxo M^{VI} types (Figures 12 and 14). The complexes **26**, **29**, **30**, and **32–34** provide

representations of site structures **5b–7b** (Figure 1) and, together with analogous tungsten complexes, allow access to oxo-transfer reactions 18 and 28. Figure 17 provides bond length comparisons between molybdenum and tungsten sites in the DMSOR family and crystallographic values for analogues of the reduced (**26**, **32**, **40**, **47**) and oxidized (**41**, **48**) sites. Protein bond lengths were determined by EXAFS analysis.^{196,209} The agreement is in general very good, in all cases ≤ 0.1 Å. Taking the analogues as unconstrained versions of the protein sites, there does not appear to be significant bond length distortion induced by protein structure. Assessment of angular distortions requires accurate protein crystal structures. We have described earlier the superposition of the W-DMSOR site and **41** and of the sulfite oxidase site and the monodithiolene complex **19**. In both cases, the analogue complexes have the same overall stereochemistry as the protein site. We conclude that the aforementioned complexes are meaningful structural analogues.

An extensive set of molybdenum and tungsten complexes has been examined by XAS using Mo K-edge and W L-edge spectra.^{160,210,211} Agreement between EXAFS and X-ray crystallographic bond lengths is excellent. The results provide an inventory of edge and EXAFS data that should prove useful in characterizing and refining metric features and structures of enzyme active sites, especially for those investigated prior to crystallographic analysis.

3.5.2. Function

The number of functional analogue systems—those that transform substrates as do enzymes (although not necessarily at comparable rates) with replicate chemical apparatus—is very small compared to the number of static structural analogues. The develop-

ment of such systems is clearly a forefront goal in the bioinorganic field. An enzyme mechanism can only be won from the enzyme. Properly designed analogue systems can reveal what is possible. Such systems have the potential of isolation and characterization of individual steps in a catalytic cycle, information that is forthcoming only by single-turnover experiments in enzyme systems. While this goal has not been achieved, there has been consequential progress in analogue reaction systems.

In non-dithiolene systems, significant advances in reactivity have been made. Systems have been developed for the molybdenum-mediated catalytic oxidation of Ph_3P by dioxygen where water is the source of the oxygen atom transferred to substrate. These systems utilize both the $\text{Mo}^{\text{IV}}\text{O}/\text{Mo}^{\text{VI}}\text{O}_2$ ^{68,69} and $\text{Mo}^{\text{IV}}/\text{Mo}^{\text{VI}}\text{O}^{140}$ reaction couples in Tp^* complexes. Water assumes this role in enzymatic reactions. Reaction 4 represents a system of broad specificity in substrate reduction, including *N*-oxide and *S*-oxide enzymatic substrates.^{59,60,62} It illustrates the use of steric hindrance in suppressing nonphysiological disproportionation reaction 3, at least in polar solvents. Protein structure eliminates this reaction in enzymes. In the reaction systems $\text{Mo}^{\text{VI}}\text{O}_2/\text{R}_3\text{P}^{75}$ and $\text{Mo}^{\text{VI}}\text{O}/\text{Ph}_3\text{P}$,¹⁴⁰ the intermediates $\text{Mo}^{\text{IV}}\text{O}(\text{OPR}_3)$ and $\text{Mo}^{\text{IV}}(\text{OPPh}_3)$, respectively, have been detected by mass spectrometry. Further, the complex $[(\text{L}^{\text{Pr}})\text{MoO}(\text{OPh})(\text{OPET}_3)]$ has been isolated and structurally characterized. Tertiary phosphines are common substrates in non-biological oxo transfer. In the present context, they simulate nucleophiles such as sulfite that are proposed to attack $\text{Mo}=\text{O}$ groups in substrate oxidation. These are examples of incomplete oxo-transfer reactions, allowing recognition of an intermediate. Crystals of *R. capsulatus* DMSOR soaked in Me_2S manifest in the X-ray structure a $\text{Me}_2\text{SO}-\text{Mo}$ interaction in an apparent intermediate in the formation of Me_2SO .²¹²

Functional aspects of bis(dithiolene) systems have been summarized (sections 3.1 and 3.2). Reaction 9 constitutes a notable result, for it was the first demonstration that a molybdenum dithiolene complex could mediate the transformation of a biological substrate. It remains now to develop monodithiolene complexes, more faithful to the SO sites **4ab** (Figure 1), which are capable of sulfite oxidation.

The most realistic functional systems are represented by reaction 23, which exhibits DMSOR and TMAOR activity. The systems utilize the $\text{M}^{\text{IV}}/\text{M}^{\text{VI}}\text{O}$ reaction couple with complexes whose ligands, especially with $\text{R} = \text{Me}$, are very closely related to the pyranopterindithiolate **1** and whose square pyramidal and distorted cis-octahedral structures are consistent with protein structural information. The phenolate ligand in complexes **26**, **40**, and **41** is a credible simulator of serinate coordination in sites **5ab**. Several interesting aspects of reactivity emerge. First, it has been reported that Mo-DMSORs such as the *E. coli* enzyme²¹³ reduce both Me_2SO and Me_3NO .²¹⁴ In contrast, *E. coli* Mo-TMAOR reduces *N*-oxides but not *S*-oxides, including Me_2SO and $(\text{CH}_2)_4\text{SO}$, at detectable rates.¹⁹⁰ However, the isoenzyme

W-TMAOR is capable of reducing both *N*-oxides and *S*-oxides (Table 7). Molybdenum complex **26** is *intrinsically competent* to reduce both substrate types, although the rate constants are very different (Table 3) and reflect another intrinsic property, the substrate rate order $\text{R}_3\text{NO} > \text{R}_2\text{SO}$ (series 38). Tungsten complex **40** reduces both types, as does the isoenzyme. Whatever is the cause of the behavior of Mo-TMAOR, it is not likely to be the inherent reactivity of the site, provided the structures **5ab** apply.

Second, the conclusion is inescapable that rates of reaction of analogue and enzyme are markedly different. Using $k_{\text{cat}}/K_{\text{M}}$ values for substrate reduction under steady-state conditions, the following values ($\text{M}^{-1} \text{s}^{-1}$) have been reported for *E. coli* enzymes and the indicated substrates:^{190,214} Me_3NO , Mo-TMAOR, 3.7×10^6 ; Me_3NO , W-TMAOR, 8.5×10^6 ; Mo-DMSOR, Me_2SO , 1.9×10^6 . Comparison with rate constants in Tables 3 and 5 indicates that enzyme rate constants are orders of magnitude greater than values for molybdenum complex **26** and tungsten complexes **39** and **40**. For *R. sphaeroides* DMSOR, resonance Raman spectroscopy indicates retention of binding of pyranopterindithiolate and serinate ligands over the catalytic cycle. It is probable that features extrinsic to the coordination unit of the catalytic site influence rates. Enzymes possess a crevice or funnel from the protein surface to the active center,^{175,212,216–218} presumably for efficient entrance of substrate and access to the active site, thus enhancing rate. It is also possible that site structure is influenced by protein structure such that it is biased toward the transition-state geometry, a point that has been raised on several occasions.^{176,203} The oxidized site **5a** in *R. sphaeroides* DMSOR is described as a distorted trigonal prism,²⁴ whereas tungsten complex **41** is nearer to the (distorted) octahedral limit.¹⁸⁰ Further, the molybdenum cofactor is held in the various proteins by a hydrogen bond network involving the pterin nucleus and phosphate–nucleotide side chains. Consequently, there are certainly environmental and possibly structural differences between analogues and enzyme sites that contribute to the large variances in rates.

Under steady-state conditions, all steps in a catalytic cycle proceed at the same rate but not necessarily with the same rate constants. With enzymes, there is very little information that allows deduction of which step—substrate binding, oxygen atom transfer, product release, or proton-coupled electron transfer—sets the turnover rate. Properly constructed analogue systems may allow separate measurement of certain steps, in particular oxo transfer and electron transfer, thereby providing information that may be useful in an eventual interpretation of enzyme mechanism. This is part of the challenge in understanding the large rate differences between the unconstrained oxo transfer executed by analogues and what we consider the highly perturbed oxo-transfer reactions of enzyme sites. The question is, what are the perturbations and how do they accelerate rates?

4. Acknowledgments

Research on biologically related molybdenum and tungsten chemistry in the authors' laboratories has been supported by NIH Grant GM 37773 (to J.H.E.) and NSF Grants 98-76457 and 02-37419 (to R.H.H.).

5. Abbreviations

Ad	2-adamantyl
AH	acetylene hydratase
AOR	aldehyde oxidoreductase
bdt	benzene-1,2-dithiolate(2 ⁻)
Bu ^t L-NS	bis(4- <i>tert</i> -butylphenyl)-2-pyridylmethanethiolate(1 ⁻)
cyt	cytochrome
DFT	density functional theory
DMSOR	dimethyl sulfoxide reductase
EDG	electron-donating group
edt	ethane-1,2-dithiolate(2 ⁻)
EPR	electron paramagnetic resonance
EWG	electron-withdrawing group
EXAFS	extended X-ray absorption fine structure
FDH	formate dehydrogenase
FMDH	<i>N</i> -formylmethanofuran dehydrogenase
L	ligand (generalized)
L'	hydrotris(3,5-dimethyl-1,2,4-triazolyl-1-yl)borate(1 ⁻)
L ^{Pr}	hydrotris(3-isopropylpyrazolyl)borate(1 ⁻)
LFER	linear free energy relationship
L-NS ₂	2,6-bis(2,2-diphenyl-2-mercaptoethyl)pyridine(2 ⁻)
L-N ₂ S ₂	<i>N,N</i> -dimethyl- <i>N,N</i> -bis(mercaptophenyl)ethylenediamine(2 ⁻)
L1OH	3- <i>tert</i> -butyl-2-hydroxy-5-methylphenyl-bis(3,5-dimethylpyrazolyl)methane
MCD	magnetic circular dichroism
Me ₂ bpy	4,4'- or 5,5'-dimethyl-2,2'-bipyridine
Me ₄ phen	3,4,7,8-tetramethyl-1,10-phenanthroline
mnt	<i>cis</i> -1,2-dicyano-1,2-ethylenedithiolate(2 ⁻) (maleonitriledithiolate(2 ⁻))
ndt	naphthalene-2,3-dithiolate(2 ⁻)
NMMO	<i>N</i> -methylmorpholine <i>N</i> -oxide
PA	proton affinity
PES	photoelectron spectroscopy
phen	1,10-phenanthroline
R ₂ C ₂ S ₂	generalized dithiolene ligand, including bdt
SCE	standard calomel electrode
SO	sulfite oxidase
SOMO	singly occupied molecular orbital
tdt	toluene-3,4-dithiolate(2 ⁻)
TMAOR	trimethylamine <i>N</i> -oxide reductase
TMSO	tetramethylenesulfoxide
Tp*	hydrotris(3,5-dimethylpyrazolyl)borate(1 ⁻)
XAS	X-ray absorption spectroscopy
XnO	xanthine oxidase

6. References

- (1) *Molybdenum and Tungsten: Their Roles in Biological Processes*, Sigel, A., Sigel, H., Eds.; Metal Ions in Biological Systems 39; Marcel Dekker: New York, 2002.
- (2) Hille, R. *Chem. Rev.* **1996**, *96*, 2757.
- (3) Hille, R. *Trends Biochem. Sci.* **2002**, *27*, 360.
- (4) Holm, R. H. *Chem. Rev.* **1987**, *87*, 1401.
- (5) Berg, J. M.; Holm, R. H. *J. Am. Chem. Soc.* **1985**, *107*, 925.
- (6) Fischer, B.; Enemark, J. H.; Basu, P. *J. Inorg. Biochem.* **1998**, *72*, 13.
- (7) Chan, M. K.; Mukund, S.; Kletzin, A.; Adams, M. W. W.; Rees, D. C. *Science* **1995**, *267*, 1463.
- (8) Dobbek, H.; Huber, R. *Met. Ions Biol. Syst.* **2002**, *39*, 227–263.
- (9) Hille, R. *Met. Ions Biol. Syst.* **2002**, *39*, 187–226.
- (10) Rajagopalan, K. V. *Adv. Enzymol. Relat. Areas Mol. Biol.* **1991**, *64*, 215.
- (11) Lorber, C.; Donahue, J. P.; Goddard, C. A.; Nordlander, E.; Holm, R. H. *J. Am. Chem. Soc.* **1998**, *120*, 8102.
- (12) Romão, M. J.; Archer, M.; Moura, I.; Moura, J. J. G.; LeGall, J.; Engh, R.; Schneider, M.; Hof, P.; Huber, R. *Science* **1995**, *270*, 1170.
- (13) Rebelo, J.; Maceira, S.; Dias, J. M.; Huber, R.; Ascenso, C. S.; Rusnak, F.; Moura, J. J. G.; Moura, I.; Romão, M. J. *J. Mol. Biol.* **2000**, *297*, 135.
- (14) Rebelo, J. M.; Dias, J. M.; Huber, R.; Moura, J. J. G.; Romão, M. J. *J. Biol. Inorg. Chem.* **2001**, *6*, 791.
- (15) Huber, R.; Hof, P.; Duarte, R. O.; Moura, J. J. G.; Moura, I.; Liu, M.-Y.; LeGall, J.; Hille, R.; Archer, M.; Romão, M. J. *Proc. Natl. Acad. Sci. U.S.A.* **1996**, *93*, 8846.
- (16) Hille, R.; George, G. N.; Eidsness, M. K.; Cramer, S. P. *Inorg. Chem.* **1989**, *28*, 4018.
- (17) Enroth, C.; Eger, B. T.; Okamoto, K.; Nishino, T.; Nishino, T.; Pai, E. F. *Proc. Natl. Acad. Sci. U.S.A.* **2000**, *97*, 10723.
- (18) Truglio, J. J.; Theis, K.; Liemkühler, S.; Rappa, R.; Rajagopalan, K. V.; Kisker, C. *Structure* **2002**, *10*, 115.
- (19) Dobbek, H.; Gremer, L.; Kiefersauer, R.; Huber, R.; Meyer, O. *Proc. Natl. Acad. Sci. U.S.A.* **2002**, *99*, 15971.
- (20) George, G. N.; Garrett, R. M.; Prince, R. C.; Rajagopalan, K. V. *J. Am. Chem. Soc.* **1996**, *118*, 8588.
- (21) Kisker, C.; Schindelin, H.; Pacheco, A.; Wehbi, W. A.; Garrett, R. M.; Rajagopalan, K. V.; Enemark, J. H.; Rees, D. C. *Cell* **1997**, *91*, 973.
- (22) George, G. N.; Pickering, I. J.; Kisker, C. *Inorg. Chem.* **1999**, *38*, 2539.
- (23) George, G. N.; Mertens, J. A.; Campbell, W. H. *J. Am. Chem. Soc.* **1999**, *121*, 9730.
- (24) Li, H.-K.; Temple, C.; Rajagopalan, K. V.; Schindelin, H. *J. Am. Chem. Soc.* **2000**, *122*, 7673.
- (25) George, G. N.; Hilton, J.; Temple, C.; Prince, R. C.; Rajagopalan, K. V. *J. Am. Chem. Soc.* **1999**, *121*, 1256.
- (26) Dias, J. M.; Than, M. E.; Humm, A.; Huber, R.; Bourenkov, G. P.; Bartunik, H. D.; Bursakov, S.; Calvete, J.; Caldeira, J.; Carneiro, C.; Moura, J. J. G.; Moura, I.; Romão, M. J. *Structure* **1999**, *7*, 65.
- (27) Boyington, J. C.; Gladyshev, V. N.; Khangulov, S. V.; Stadtman, T. C.; Sun, P. D. *Science* **1997**, *275*, 1305.
- (28) Jormakka, M.; Törnroth, S.; Byrne, B.; Iwata, S. *Science* **2002**, *295*, 1863.
- (29) George, G. N.; Colangelo, C. M.; Dong, J.; Scott, R. A.; Khangulov, S. V.; Gladyshev, V. N.; Stadtman, T. C. *J. Am. Chem. Soc.* **1998**, *120*, 1267.
- (30) George, G. N.; Costa, C.; Moura, J. J. G.; Moura, I. *J. Am. Chem. Soc.* **1999**, *121*, 2625.
- (31) Roy, R.; Adams, M. W. W. *Met. Ions Biol. Syst.* **2002**, *39*, 673.
- (32) L'vov, N. P.; Nosikov, A. N.; Antipov, A. N. *Biochemistry (Moscow)* **2002**, *67*, 234.
- (33) Holm, R. H. *Coord. Chem. Rev.* **1990**, *100*, 183.
- (34) Enemark, J. H.; Young, C. G. *Adv. Inorg. Chem.* **1994**, *40*, 1.
- (35) Bradshaw, B.; Dinsmore, A.; Ajana, W.; Collison, D.; Garner, C. D.; Joule, J. A. *J. Chem. Soc., Perkin Trans.* **2001**, *24*, 3239.
- (36) Collison, D.; Garner, C. D.; Joule, J. A. *Chem. Soc. Rev.* **1996**, *25*.
- (37) Fischer, B.; Burgmayer, S. J. N. *Met. Ions Biol. Syst.* **2002**, *39*, 265.
- (38) *Molybdenum Enzymes*; Spiro, T. G., Ed.; John Wiley & Sons: New York, 1985.
- (39) *Molybdenum Enzymes, Cofactors, and Model Systems*; Stiefel, E. I., Coucouvanis, D., Newton, W. E., Eds.; ACS Symposium Series 535; American Chemical Society: Washington, DC, 1993.
- (40) Pilato, R. S.; Stiefel, E. I. In *Bioinorganic Catalysis*; Reedijk, J., Bouwman, E., Eds.; Marcel Dekker: New York, 1999; pp 81–152.
- (41) Hille, R.; Rétey, J.; Bartlewski-Hof, U.; Reichenbecher, W.; Schink, B. *FEMS Microbiol. Rev.* **1999**, *22*, 489.
- (42) Stiefel, E. I. *J. Chem. Soc., Dalton Trans.* **1997**, 3915.
- (43) Young, C. G.; Wedd, A. G. *J. Chem. Soc., Chem. Commun.* **1997**, 1251.
- (44) Young, C. J. *J. Biol. Inorg. Chem.* **1997**, *2*, 810.
- (45) Lim, B. S.; Fomitchev, D. V.; Holm, R. H. *Inorg. Chem.* **2001**, *40*, 4257.
- (46) Mader, M. L.; Carducci, M. D.; Enemark, J. H. *Inorg. Chem.* **2000**, *39*, 525.
- (47) Dowerah, D.; Spence, J. T.; Singh, R.; Wedd, A. G.; Wilson, G. L.; Farchione, F.; Enemark, J. H.; Kristofzski, J.; Bruck, M. J. *Am. Chem. Soc.* **1987**, *109*, 5655.
- (48) Singh, R.; Spence, J. T.; George, G. N.; Cramer, S. P. *Inorg. Chem.* **1989**, *28*, 8.
- (49) Barnard, K. R.; Bruck, M.; Huber, S.; Grittini, C.; Enemark, J. H.; Gable, R. W.; Wedd, A. G. *Inorg. Chem.* **1997**, *36*, 637.
- (50) McNaughton, R. L.; Helton, M. E.; Cosper, M. M.; Enemark, J. H.; Kirk, M. L., *Inorg. Chem.*, in press.
- (51) Dhawan, I.; Enemark, J. H. *Inorg. Chem.* **1996**, *35*, 4873.

- (52) Garner, C. D.; Charnock, J. M. In *Comprehensive Coordination Chemistry*, Vol. 3; Wilkinson, G., Gillard, R. D., McCleverty, J. A., Eds.; Pergamon Press: New York, 1987; pp 1329–1374.
- (53) Stiefel, E. I. In *Comprehensive Coordination Chemistry*, Vol. 3; Wilkinson, G., Gillard, R. D., McCleverty, J. A., Eds.; Pergamon Press: New York, 1987; pp 1375–1420.
- (54) Garner, C. D. In *Comprehensive Coordination Chemistry*, Vol. 3; Wilkinson, G., Gillard, R. D., McCleverty, J. A., Eds.; Pergamon Press: New York, 1987; pp 1421–1444.
- (55) Dori, Z. In *Comprehensive Coordination Chemistry*, Vol. 3; Wilkinson, G., Gillard, R. D., McCleverty, J. A., Eds.; Pergamon Press: New York, 1987; pp 973–1022.
- (56) Craig, J. A.; Harlan, E. W.; Snyder, B. S.; Whitener, M. A.; Holm, R. H. *Inorg. Chem.* **1989**, *28*, 2082.
- (57) Berg, J. M.; Holm, R. H. *J. Am. Chem. Soc.* **1985**, *107*, 917.
- (58) Doonan, C. J.; Slizys, D. A.; Young, C. G. *J. Am. Chem. Soc.* **1999**, *121*, 6430.
- (59) Gheller, S. F.; Schultz, B. E.; Scott, M. J.; Holm, R. H. *J. Am. Chem. Soc.* **1992**, *114*, 6934.
- (60) Schultz, B. E.; Gheller, S. F.; Muetterties, M. C.; Scott, M. J.; Holm, R. H. *J. Am. Chem. Soc.* **1993**, *115*, 2714.
- (61) Holm, R. H.; Donahue, J. P. *Polyhedron* **1993**, *12*, 571.
- (62) Schultz, B. E.; Holm, R. H. *Inorg. Chem.* **1993**, *32*, 4244.
- (63) Pietsch, M. A.; Hall, M. B. *Inorg. Chem.* **1996**, *35*, 1273.
- (64) Izumi, Y.; Glaser, T.; Rose, K.; McMaster, J.; Basu, P.; Enemark, J. H.; Hedman, B.; Hodgson, K. O.; Solomon, E. I. *J. Am. Chem. Soc.* **1999**, *121*, 10035.
- (65) Žmirić, A.; Zarić, S. D. *Inorg. Chem. Commun.* **2002**, *5*, 446.
- (66) Thomsson, L. M.; Hall, M. B. *J. Am. Chem. Soc.* **2001**, *123*, 3995.
- (67) Rappé, A. K.; Goddard, W. A., III. *J. Am. Chem. Soc.* **1982**, *104*, 3287.
- (68) Xiao, Z.; Young, C. G.; Enemark, J. H.; Wedd, A. G. *J. Am. Chem. Soc.* **1992**, *114*, 9194.
- (69) Xiao, Z.; Bruck, M. A.; Enemark, J. H.; Young, C. G.; Wedd, A. G. *Inorg. Chem.* **1996**, *35*, 7508.
- (70) Roberts, S. A.; Young, C. G.; Cleland, W. E., Jr.; Ortega, R. B.; Enemark, J. H. *Inorg. Chem.* **1988**, *27*, 3044.
- (71) Xiao, Z.; Bruck, M.; Doyle, C.; Enemark, J. H.; Grittini, C.; Gable, R. W.; Wedd, A. G.; Young, C. G. *Inorg. Chem.* **1995**, *34*, 5950.
- (72) Bray, R. C. *Polyhedron* **1986**, *5*, 591.
- (73) Xiao, Z.; Gable, R. W.; Wedd, A. G.; Young, C. G. *J. Am. Chem. Soc.* **1996**, *118*, 2912.
- (74) Xiao, Z.; Gable, R. W.; Wedd, A. G.; Young, C. G. *J. Chem. Soc., Chem. Commun.* **1994**, 1295.
- (75) Smith, P. D.; Millar, A. J.; Young, C. G.; Ghosh, A.; Basu, P. *J. Am. Chem. Soc.* **2000**, *122*, 9298.
- (76) Roberts, S. A.; Young, C. G.; Kipke, C. A.; Cleland, W. E., Jr.; Yamanouchi, K.; Carducci, M. D.; Enemark, J. H. *Inorg. Chem.* **1990**, *29*, 3650.
- (77) Millar, A. J.; Doonan, C. J.; Laughlin, L. J.; Tiekink, E. R. T.; Young, C. G. *Inorg. Chim. Acta* **2002**, *337*, 393.
- (78) Laughlin, L. J.; Young, C. G. *Inorg. Chem.* **1996**, *35*, 1050.
- (79) Young, C. G.; Laughlin, L. J.; Colmanet, S.; Scrofanì, S. D. B. *Inorg. Chem.* **1996**, *35*, 5368.
- (80) Cleland, W. E., Jr.; Barnhart, K. M.; Yamanouchi, K.; Ortega, R. B.; Enemark, J. H. *Inorg. Chem.* **1987**, *26*, 1017.
- (81) McNaughton, R. L.; Tipton, A. A.; Rubie, N. D.; Conry, R. R.; Kirk, M. L. *Inorg. Chem.* **2000**, *39*, 5967.
- (82) Peariso, K.; McNaughton, R. L.; Kirk, M. L. *J. Am. Chem. Soc.* **2002**, *124*, 9006.
- (83) Carducci, M. D.; Brown, C.; Solomon, E. I.; Enemark, J. H. *J. Am. Chem. Soc.* **1994**, *116*, 11856.
- (84) Inscore, F. E.; McNaughton, R. L.; Westcott, B.; Helton, M. E.; Jones, R.; Dhawan, I. K.; Enemark, J. H.; Kirk, M. L. *Inorg. Chem.* **1999**, *38*, 1401.
- (85) Inscore, F. E.; Joshi, H. K.; McElhaney, A. E.; Enemark, J. H. *Inorg. Chim. Acta* **2002**, *331*, 246.
- (86) Mabbs, F. E.; Collison, D. *Electron Paramagnetic Resonance of d Transition Metal Compounds*; Elsevier: Amsterdam, 1992.
- (87) Westcott, B. L.; Gruhn, N. E.; Enemark, J. H. *J. Am. Chem. Soc.* **1998**, *120*, 3382.
- (88) Westcott, B. L.; Enemark, J. H. *Inorg. Chem.* **1997**, *36*, 5404.
- (89) Helton, M. E.; Gruhn, N. E.; McNaughton, R. L.; Kirk, M. L. *Inorg. Chem.* **2000**, *39*, 2273.
- (90) McElhaney, A. E.; Inscore, F. E.; Schirlin, J. T.; Enemark, J. H. *Inorg. Chim. Acta* **2002**, *341*, 85.
- (91) Lauher, J. W.; Hoffman, R. J. *J. Am. Chem. Soc.* **1976**, *98*, 1729.
- (92) Inscore, F. E.; Rubie, N. D.; Joshi, H. K.; Kirk, M. L.; Enemark, J. H., submitted for publication.
- (93) Joshi, H. K.; Cooney, J. J. A.; Inscore, F. E.; Gruhn, N. E.; Lichtenberger, D. L.; Enemark, J. H. *Proc. Natl. Acad. Sci. U.S.A.* **2003**, *100*, 3719.
- (94) Enemark, J. H.; Westcott, B. L. In *Inorganic Electronic Structure and Spectroscopy, Vol. II: Applications and Case Studies*; Solomon, E. I., Lever, A. B. P., Eds.; John Wiley and Sons: New York, 1999; pp 403–450.
- (95) Kutoglu, A.; Köpf, H. *J. Organomet. Chem.* **1970**, *25*, 455.
- (96) Palanca, P.; Picher, T.; Sanz, V.; Gómez-Romero, P.; Llopis, E.; Domenech, A.; Cervilla, A. *J. Chem. Soc., Chem. Commun.* **1990**, 531.
- (97) Sanz, V.; Picher, T.; Palanca, P.; Gómez-Romero, P.; Llopis, E.; Ramirez, J. A.; Beltrán, D.; Cervilla, A. *Inorg. Chem.* **1991**, *30*, 3113.
- (98) Cervilla, A.; Ramirez, J. A.; Llopis, E.; Palanca, P. *Inorg. Chem.* **1993**, *32*, 2085.
- (99) Cervilla, A.; Doménech, A.; Llopis, E.; Vicente, F.; Tamarit, R. *Inorg. Chim. Acta* **1994**, *221*, 117.
- (100) Cervilla, A.; Corma, A.; Fornés, V.; Llopis, E.; Palanca, P.; Rey, F.; Ribera, A. *J. Am. Chem. Soc.* **1994**, *116*, 1595.
- (101) Cervilla, A.; Corma, A.; Fornés, V.; Pérez, F.; Rey, F.; Ribera, A. *J. Am. Chem. Soc.* **1995**, *117*, 6781.
- (102) Corma, A.; Rey, F.; Thomas, J. M.; Sankar, G.; Greaves, G. N.; Cervilla, A.; Llopis, E.; Ribeira, A. *J. Chem. Soc., Chem. Commun.* **1996**, 1613.
- (103) Arzoumanian, H.; Lopez, R.; Agrifoglio, G. *Inorg. Chem.* **1994**, *33*, 31779.
- (104) Thapper, A.; Donahue, J. P.; Musgrave, K. B.; Willer, M. W.; Nordlander, E.; Hedman, B.; Hodgson, K. O.; Holm, R. H. *Inorg. Chem.* **1999**, *38*, 4104.
- (105) Miao, M.; Willer, M. W.; Holm, R. H. *Inorg. Chem.* **2000**, *39*, 2843.
- (106) Smith, P. D.; Slizys, D. A.; George, G. N.; Young, C. G. *J. Am. Chem. Soc.* **2000**, *122*, 2946.
- (107) Eagle, A. A.; Harben, S. M.; Tiekink, E. R. T.; Young, C. G. *J. Am. Chem. Soc.* **1994**, *116*, 9749.
- (108) Faller, J. W.; Ma, Y. *Organometallics* **1989**, *8*, 609.
- (109) Hofer, E.; Holzbach, W.; Wieghardt, K. *Angew. Chem., Int. Ed. Engl.* **1981**, *20*, 282.
- (110) Coucouvanis, D.; Toupadakis, A.; Lane, J. D.; Koo, S.-M.; Kim, C. G.; Hadjikyriacou, A. *J. Am. Chem. Soc.* **1991**, *113*, 5271.
- (111) Coucouvanis, D. *Adv. Inorg. Chem.* **1997**, *45*, 1.
- (112) Eagle, A. A.; Laughlin, L. J.; Young, C. G.; Tiekink, E. R. T. *J. Am. Chem. Soc.* **1992**, *114*, 9195.
- (113) Bray, R. C. *Q. Rev. Biophys.* **1988**, *21*, 299.
- (114) Farchione, F.; Hanson, G. R.; Rodrigues, C. F.; Bailey, T. D.; Bagchi, R. N.; Bond, A. M.; Pilbrow, J. R.; Wedd, A. G. *J. Am. Chem. Soc.* **1986**, *108*, 831.
- (115) Wilson, G. L.; Kony, M.; Tiekink, E. R. T.; Pilbrow, J. R.; Spence, J. T.; Wedd, A. G. *J. Am. Chem. Soc.* **1988**, *110*, 6923.
- (116) Wilson, G. L.; Greenwood, R. J.; Pilbrow, J. R.; Spence, J. T.; Wedd, A. G. *J. Am. Chem. Soc.* **1991**, *113*, 6803.
- (117) Hinshaw, C. J.; Peng, G.; Singh, R.; Spence, J. T.; Enemark, J. H.; Bruck, M.; Kristofzski, J.; Merbs, S. L.; Ortega, R. B.; Wexler, P. A. *Inorg. Chem.* **1989**, *28*, 4483.
- (118) Peng, G.; Nichols, J.; McCullough, E. A. J.; Spence, J. T. *Inorg. Chem.* **1994**, *33*, 2857.
- (119) Waldron, K. A.; Topich, J. J. *Inorg. Biochem.* **1997**, *66*, 271.
- (120) Bray, R. C.; Gutteridge, S.; Stotter, D.; Tanner, S. J. *Biochem. J.* **1979**, *177*, 357.
- (121) Young, C. G.; Enemark, J. H.; Collison, D.; Mabbs, F. E. *Inorg. Chem.* **1987**, *26*, 2925.
- (122) Johnson, A. R.; Davis, W. M.; Cummins, C. C.; Serron, S.; Nolan, S. P.; Musaev, D. G.; Morokuma, K. *J. Am. Chem. Soc.* **1998**, *120*, 2071.
- (123) Boyd, I.; Dance, I. G.; Murray, K. S.; Wedd, A. G. *Aust. J. Chem.* **1978**, *31*, 279.
- (124) Bradbury, J. R.; Mackay, M. F.; Wedd, A. G. *Aust. J. Chem.* **1978**, *31*, 2423.
- (125) Conry, R. R.; Tipton, A. A. *J. Biol. Inorg. Chem.* **2001**, *6*, 359.
- (126) McMaster, J.; Carducci, M. D.; Yang, Y.-S.; Solomon, E. I.; Enemark, J. H. *Inorg. Chem.* **2001**, *40*, 687.
- (127) Boyde, S.; Ellis, S. R.; Garner, C. D.; Clegg, W. *J. Chem. Soc., Chem. Commun.* **1986**, 1541.
- (128) Ellis, S. R.; Collison, D.; Garner, C. D.; Clegg, W. *J. Chem. Soc., Chem. Commun.* **1986**, 1483.
- (129) Wang, X.-B.; Inscore, F. E.; Yang, X.; Cooney, J. J. A.; Enemark, J. H.; Wang, L.-S. *J. Am. Chem. Soc.* **2002**, *124*, 10182.
- (130) Donahue, J. P.; Goldsmith, C. R.; Nadiminti, U.; Holm, R. H. *J. Am. Chem. Soc.* **1998**, *120*, 12869.
- (131) McNaughton, R. L.; Helton, M. E.; Rubie, N. D.; Kirk, M. L. *Inorg. Chem.* **2000**, *39*, 4386.
- (132) Ellis, S. R.; Collison, D.; Garner, C. D. *J. Chem. Soc., Dalton Trans.* **1989**, 413.
- (133) Kondo, M.; Ueyama, N.; Fukuyama, K.; Nakamura, A. *Bull. Chem. Soc. Jpn.* **1993**, *66*, 1391.
- (134) Ueyama, N.; Okamura, T.; Nakamura, A. *J. Am. Chem. Soc.* **1992**, *114*, 8129.
- (135) Mondal, S.; Basu, P. *Inorg. Chem.* **2001**, *40*, 192.
- (136) Davie, S. R.; Rubie, N. D.; Hammes, B. S.; Carrano, C. J.; Kirk, M. L.; Basu, P. *Inorg. Chem.* **2001**, *40*, 2632.
- (137) Enemark, J. H.; Cospér, M. M. *Met. Ions Biol. Syst.* **2002**, *39*, 621.
- (138) Mondal, J. U.; Schultz, F. A.; Brennan, T. D.; Scheidt, W. R. *Inorg. Chem.* **1988**, *27*, 3950.
- (139) Arzoumanian, H.; Corao, C.; Krentzien, H.; Lopez, R.; Teruel, H. *J. Chem. Soc., Chem. Commun.* **1992**, 856.

- (140) Nemykin, V. N.; Davie, S. R.; Mondal, S.; Rubie, N.; Kirk, M. L.; Somogyi, A.; Basu, P. *J. Am. Chem. Soc.* **2002**, *124*, 756.
- (141) Johnson, M. K.; Rees, D. C.; Adams, M. W. W. *Chem. Rev.* **1996**, *96*, 2817.
- (142) Mukund, S.; Adams, M. W. W. *J. Biol. Chem.* **1991**, *266*, 14208.
- (143) George, G. N.; Prince, R. C.; Mukund, S.; Adams, M. W. W. *J. Am. Chem. Soc.* **1992**, *114*, 3521.
- (144) Barnard, K. R.; Gable, R. W.; Wedd, A. G. *J. Biol. Inorg. Chem.* **1997**, *2*, 623.
- (145) Cervilla, A.; Llopis, E.; Ribera, A.; Doménech, A.; Sinn, E. *J. Chem. Soc., Dalton Trans.* **1994**, *23*, 3511.
- (146) Eagle, A. A.; Tiekink, E. R. T.; Young, C. G. *J. Chem. Soc., Chem. Commun.* **1991**, 1746.
- (147) Tucci, G. C.; Donahue, J. P.; Holm, R. H. *Inorg. Chem.* **1998**, *37*, 1602.
- (148) Schroth, W.; Peschel, J. *Chimia* **1964**, *18*, 171.
- (149) Davison, A.; Holm, R. H. *Inorg. Synth.* **1967**, *10*, 8.
- (150) Tian, Z.-Q.; Donahue, J. P.; Holm, R. H. *Inorg. Chem.* **1995**, *34*, 5567.
- (151) Schrauzer, G. N.; Mayweg, V. P. *J. Am. Chem. Soc.* **1965**, *87*, 1483.
- (152) Sung, K.-M.; Holm, R. H. *J. Am. Chem. Soc.* **2002**, *124*, 4312.
- (153) Davies, E. S.; Beddoes, R. L.; Collison, D.; Dinsmore, A.; Docrat, A.; Joule, J. A.; Wilson, C. R.; Garner, C. D. *J. Chem. Soc., Dalton Trans.* **1997**, 3985.
- (154) Davies, E. S.; Aston, G. M.; Beddoes, R. L.; Collison, D.; Dinsmore, A.; Docrat, A.; Joule, J. A.; Wilson, C. R.; Garner, C. D. *J. Chem. Soc., Dalton Trans.* **1998**, 3647.
- (155) Goddard, C. A.; Holm, R. H. *Inorg. Chem.* **1999**, *38*, 5389.
- (156) Lim, B. S.; Donahue, J. P.; Holm, R. H. *Inorg. Chem.* **2000**, *39*, 263.
- (157) McCleverty, J. A. *Prog. Inorg. Chem.* **1968**, *10*, 49.
- (158) Johnson, J. L.; Rajagopalan, K. V. *Proc. Natl. Acad. Sci. U.S.A.* **1982**, *79*, 6856.
- (159) Lim, B. S.; Willer, M. W.; Miao, M.; Holm, R. H. *J. Am. Chem. Soc.* **2001**, *123*, 8343.
- (160) Jalilvand, F.; Lim, B. S.; Holm, R. H.; Hedman, B.; Hodgson, K. O. *Inorg. Chem.* **2003**, *42*, 5531.
- (161) Dhawan, I.; Pacheco, A.; Enemark, J. H. *J. Am. Chem. Soc.* **1994**, *116*, 7911.
- (162) Das, S. K.; Chaudhury, P. K.; Biswas, D.; Sarkar, S. *J. Am. Chem. Soc.* **1994**, *116*, 9061.
- (163) Lorber, C.; Plutino, M. R.; Elding, L. I.; Nordlander, E. *J. Chem. Soc., Dalton Trans.* **1997**, 3997.
- (164) Chaudhury, P. K.; Das, S. K.; Sarkar, S. *Biochem. J.* **1996**, *319*, 953.
- (165) Oku, H.; Ueyama, N.; Kondo, M.; Nakamura, A. *Inorg. Chem.* **1994**, *33*, 209.
- (166) Oku, H.; Ueyama, N.; Nakamura, A. *Inorg. Chem.* **1997**, *36*, 1504.
- (167) Ansari, M. A.; Chandrasekaran, J.; Sarkar, S. *Inorg. Chim. Acta* **1987**, *133*, 133.
- (168) Coucouvanis, D.; Hadjikyriacou, A.; Toupadakis, A.; Koo, S.-M.; Ileperuma, O.; Draganjac, M.; Salifoglou, A. *Inorg. Chem.* **1991**, *30*, 754.
- (169) Matsubayashi, G.; Nojo, T.; Tanaka, T. *Inorg. Chim. Acta* **1988**, *154*, 133.
- (170) Götz, B.; Knoch, F.; Kisch, H. *Chem. Ber.* **1996**, *129*, 33.
- (171) McCleverty, J. A.; Locke, J.; Ratcliff, B.; Wharton, E. J. *Inorg. Chim. Acta* **1969**, *3*, 283.
- (172) Ueyama, N.; Oku, H.; Kondo, M.; Okamura, T.; Yoshinaga, N.; Nakamura, A. *Inorg. Chem.* **1996**, *35*, 643.
- (173) Oku, H.; Ueyama, N.; Nakamura, A. *Inorg. Chem.* **1995**, *34*, 3667.
- (174) Schultz, B. E.; Holm, R. H.; Hille, R. *J. Am. Chem. Soc.* **1995**, *117*, 827.
- (175) Czjzek, M.; Dos Santos, J.-P.; Pommier, J.; Méjean, V.; Haser, R. *J. Mol. Biol.* **1998**, *284*, 435.
- (176) Lim, B. S.; Holm, R. H. *J. Am. Chem. Soc.* **2001**, *123*, 1920.
- (177) Schrauzer, G. N.; Mayweg, V. P.; Heinrich, W. *J. Am. Chem. Soc.* **1966**, *88*, 5174.
- (178) Fomitchev, D. V.; Lim, B. S.; Holm, R. H. *Inorg. Chem.* **2001**, *40*, 645.
- (179) Lim, B. S.; Sung, K.-M.; Holm, R. H. *J. Am. Chem. Soc.* **2000**, *122*, 7410.
- (180) Sung, K.-M.; Holm, R. H. *J. Am. Chem. Soc.* **2001**, *123*, 1931.
- (181) Sung, K.-M.; Holm, R. H. *Inorg. Chem.* **2001**, *40*, 4518.
- (182) Acree, W. E., Jr.; Tucker, S. A.; Ribeiro da Silva, M. D. M. C.; Matos, M. A. R.; Gonçalves, J. M.; Ribeiro da Silva, Pilcher, G. *J. Chem. Thermodyn.* **2000**, *27*, 391.
- (183) Kletzin, A.; Adams, M. W. W. *FEMS Microbiol. Rev.* **1996**, *18*, 5.
- (184) Garner, C. D.; Stewart, L. J. *Met. Ions Biol. Syst.* **2002**, *39*, 699.
- (185) Meckenstock, R. U.; Krieger, R.; Kroneck, P. M. H.; Schink, B. *Eur. J. Biochem.* **1999**, *264*, 176.
- (186) Beinert, H.; Kennedy, M. C.; Stout, C. D. *Chem. Rev.* **1996**, *96*, 2335.
- (187) Hu, Y.; Faham, S.; Roy, R.; Adams, M. W. W.; Rees, D. C. *J. Mol. Biol.* **1999**, *286*, 899.
- (188) Raaijmakers, H.; Teixeira, S.; Dias, J. M.; Almendra, M. J.; Brondino, C. D.; Moura, I.; Moura, J. J. G.; Romão, M. J. *J. Biol. Inorg. Chem.* **2001**, *6*, 398.
- (189) Raaijmakers, H.; Macieira, S.; Dias, J. M.; Teixeira, S.; Bursakov, S.; Huber, R.; Moura, J. J. G.; Moura, I.; Romão, M. J. *Structure* **2002**, *10*, 1261.
- (190) Buc, J.; Santini, C.-L.; Giordani, R.; Czjzek, M.; Wu, L.-F.; Giordano, G. *Mol. Microbiol.* **1999**, *32*, 159.
- (191) Sarkar, S.; Das, S. K. *Proc. Indian Acad. Sci. (Chem. Sci.)* **1992**, *104*, 533.
- (192) Ueyama, N.; Oku, H.; Nakamura, A. *J. Am. Chem. Soc.* **1992**, *114*, 7310.
- (193) Das, S. K.; Biswas, D.; Maiti, R.; Sarkar, S. *J. Am. Chem. Soc.* **1996**, *118*, 1387.
- (194) Oku, H.; Ueyama, N.; Nakamura, A. *Bull. Chem. Soc. Jpn.* **1996**, *69*, 3139.
- (195) Sung, K.-M.; Holm, R. H. *Inorg. Chem.* **2000**, *39*, 1275.
- (196) Stewart, L. J.; Bailey, S.; Bennett, B.; Charnock, J. M.; Garner, C. D.; McAlpine, A. S. *J. Mol. Biol.* **2000**, *299*, 593.
- (197) Caradonna, J. P.; Reddy, P. R.; Holm, R. H. *J. Am. Chem. Soc.* **1988**, *110*, 2139.
- (198) Craig, J. A.; Holm, R. H. *J. Am. Chem. Soc.* **1989**, *111*, 2111.
- (199) Bhattacharjee, S.; Bhattacharyya, R. *J. Chem. Soc., Dalton Trans.* **1993**, 1151.
- (200) Baird, D. M.; Aburri, C.; Barron, L. S.; Rodriguez, S. A. *Inorg. Chim. Acta* **1995**, *237*, 117.
- (201) Thapper, A.; Deeth, R. J.; Nordlander, E. *Inorg. Chem.* **1999**, *38*, 1015.
- (202) Reynolds, M. S.; Berg, J. M.; Holm, R. H. *Inorg. Chem.* **1984**, *23*, 3057.
- (203) Webster, C. E.; Hall, M. B. *J. Am. Chem. Soc.* **2001**, *123*, 5820.
- (204) Schmitz, R. A.; Richter, M.; Linder, D.; Thauer, R. K. *Eur. J. Biochem.* **1992**, *207*, 559.
- (205) Bertram, P. A.; Schmitz, R.; Linder, D.; Thauer, R. K. *Arch. Microbiol.* **1994**, *161*, 220.
- (206) Bertram, P. A.; Karrasch, M.; Schmitz, R. A.; Böcher, R.; Albracht, S. P. J.; Thauer, R. K. *Eur. J. Biochem.* **1994**, *220*, 477.
- (207) Thapper, A.; Deeth, R. J.; Nordlander, E. *Inorg. Chem.* **2002**, *41*, 6695.
- (208) Ellis, P. J.; Conrads, T.; Hille, R.; Kuhn, P. *Structure* **2001**, *9*, 125.
- (209) George, G. N.; Hilton, J.; Rajagopalan, K. V. *J. Am. Chem. Soc.* **1996**, *118*, 1113.
- (210) Musgrave, K. B.; Donahue, J. P.; Lorber, C.; Holm, R. H.; Hedman, B.; Hodgson, K. O. *J. Am. Chem. Soc.* **1999**, *121*, 10297.
- (211) Musgrave, K. B.; Lim, B. S.; Sung, K.-M.; Holm, R. H.; Hedman, B.; Hodgson, K. O. *Inorg. Chem.* **2000**, *39*, 5238.
- (212) McAlpine, A. S.; McEwan, A. G.; Bailey, S. *J. Mol. Biol.* **1998**, *275*, 613.
- (213) Simala-Grant, J. L.; Weiner, J. H. *Eur. J. Biochem.* **1998**, *251*, 510.
- (214) Adams, B.; Smith, A. T.; Bailey, S.; McEwan, A. G.; Bray, R. C. *Biochemistry* **1999**, *38*, 8501.
- (215) Garton, S. D.; Hilton, J.; Oku, H.; Crouse, B. R.; Rajagopalan, K. V.; Johnson, M. K. *J. Am. Chem. Soc.* **1997**, *119*, 12906.
- (216) Schindelin, H.; Kisker, C.; Hilton, J.; Rajagopalan, K. V.; Rees, D. C. *Science* **1996**, *272*, 1615.
- (217) Schneider, F.; Löwe, J.; Huber, R.; Schindelin, H.; Kisker, C.; Knäblein, J. *J. Mol. Biol.* **1996**, *263*, 53.
- (218) McAlpine, A. S.; McEwan, A. G.; Shaw, A. L.; Bailey, S. *J. Biol. Inorg. Chem.* **1997**, *2*, 690.

CR020609D